Forschungszentrum Karlsruhe
in der Helmholtz-Gemeinschaft

Wissenschaftliche Berichte
FZKA 7178

FLUENT Simulations for THERESA Facility

Z. Xu, A. Kotchourko, L. Krebs, W. Breitung

Institut für Kern- und Energietechnik
Programm Nachhaltigkeit und Technik

Oktober 2005

Forschungszentrum Karlsruhe

in der Helmholtz-Gemeinschaft

Wissenschaftliche Berichte

FZKA 7178

FLUENT Simulations for THERESA Facility

Z. Xu, A. Kotchourko, L. Krebs, W. Breitung

Institut für Kern- und Energietechnik

Programm Nachhaltigkeit und Technik

Forschungszentrum Karlsruhe GmbH, Karlsruhe
2005

Impressum der Print-Ausgabe:

Als Manuskript gedruckt

Forschungszentrum Karlsruhe GmbH
Postfach 3640, 76021 Karlsruhe

Mitglied der Hermann von Helmholtz-Gemeinschaft
Deutscher Forschungszentren (HGF)

ISSN 0947-8620

urn:nbn:de:0005-071789

Abstract

FLUENT Simulations for THERESA Facility

Numerical calculations have been performed by using the computer code FLUENT to simulate theoretically the flow field and the temperature distribution in the THERESA facility, an experimental equipment simulating a realistic waste combustor. A finite element model about the whole geometry containing half million cells is applied in the simulations. The eddy-dissipation model is applied to simulate the turbulent combustion occurring in the combustor. The simulations indicate that the acute chemical reactions of fuel/oxidant take place essentially in the first half of the combustion chamber, and that the wall temperature of the other half decreases owing to thermal radiations. The influence of different wall boundary conditions of the compartment between the combustion chamber and the post-combustion chamber on the flow field in this domain has been studied. The computational results manifest that the change of boundary conditions does not result in a noticeable difference in the axial temperature of the combustion chamber. The influence of activated or deactivated cooling system is investigated too. The numerical results show that the axial temperature decrease caused by the cooling system does not exceed 11 K at the exit of the combustor. The cooling effect of evaporation of the water trap is modeled also. Calculations manifest that this factor does not decrease considerably the temperature at the exit of the burner either. In summary, the three accounted factors do not play key roles on the temperature distribution at the exit of the combustion chamber.

Kurzfassung

FLUENT Simulation für die THERESA Anlage

Die THERESA Anlage ist ein experimenteller Teststand, um eine realistische Abfall Verbrennung zu simulieren. Um das Strömungsfeld und die Temperaturverteilung in der THERESA Anlage darzustellen, wurden mit Hilfe des Rechencodes FLUENT numerische Kalkulationen durchgeführt. In der Rechensimulation wurde für die gesamte enthaltene Geometrie ein Finites Element Modell mit einer halben Million Zellen angelegt. Das Eddy-Dissipationsmodell wurde zur Anwendung gebracht, um den in Erscheinung tretenden turbulenten Abbrand im Verbrennungsraum nachzustellen. Die Simulation stellt die heftige chemische Reaktion von Brennstoff/Oxidationsmittel dar, welche im Wesentlichen in der ersten Hälfte des Verbrennungsraums stattfindet. Ebenso ist hierin berücksichtigt, dass die Wandtemperatur der zweiten Brennkammerhälfte durch thermische Abstrahlung gemindert wird. Hierbei wurde der Einfluss auf das Strömungsfeld im Arbeitsbereich, auf Grund des Einflusses von unterschiedlichen Grenzflächenbedingungen der angrenzenden Verbrennungskammer und der Nachbrennkammer, untersucht. Die mittels des benannten Programms durchgeführten Berechnungen ergaben, dass der Wechsel der Grenzflächen-bedingungen sich nicht in einer bemerkenswerten Differenz der axialen Temperatur der Verbrennungskammer manifestiert. Ebenso wurde der Einfluss eines zugeschalteten oder deaktivierten Kühlsystems untersucht. Die numerischen Ergebnisse zeigten, dass auf Grund des eingesetzten Kühlsystems die axiale Temperatur einen Wert von 11 K im Austritt der Verbrennungskammer nicht überschreitet. Im Weiteren wurde der Kühleinfluss durch die Verdampfung am Wasserabscheider modelliert. Die Berechnungen hierzu ergaben, dass dieser Einfluss die Temperatur am Austritt des Brennraums nicht wesentlich absenkt. Im Gesamten lässt sich hieraus schließen, dass die benannten drei Faktoren keine Schlüsselrolle für die Temperaturverteilung am Austritt der Verbrennungskammer darstellen.

CONTENTS

1. Introduction

THERESA is an experimental facility in a large scale in FZK modeling a waste combustor in industry. The facility consists of a rotary kiln of about ten meters in length and an up-standing post-combustion chamber (PCC) of about thirteen meters in height. The kiln rotates one turn in every minute. Wastes with additional fuel are burnt in the rotary kiln into gas products and ashes, which are separated in the PCC. The gas products, which could pollute the environment, are discharged through the outlet on the top of the PCC, and are conducted into a post-processing system. The ashes are deposited into a water sink on the bottom of the PCC, and cool down in it. The engineering drawing patches of THERESA are put together in Figure 1.1. In order to protect the metal structure from high temperatures, a cooling system is constructed at the compartment between the rotary kiln and the PCC, which is a cylindrical hollow wrap around the exit of the rotary kiln. The structure is cooled by cold air vented into the annular space by eight nozzles.

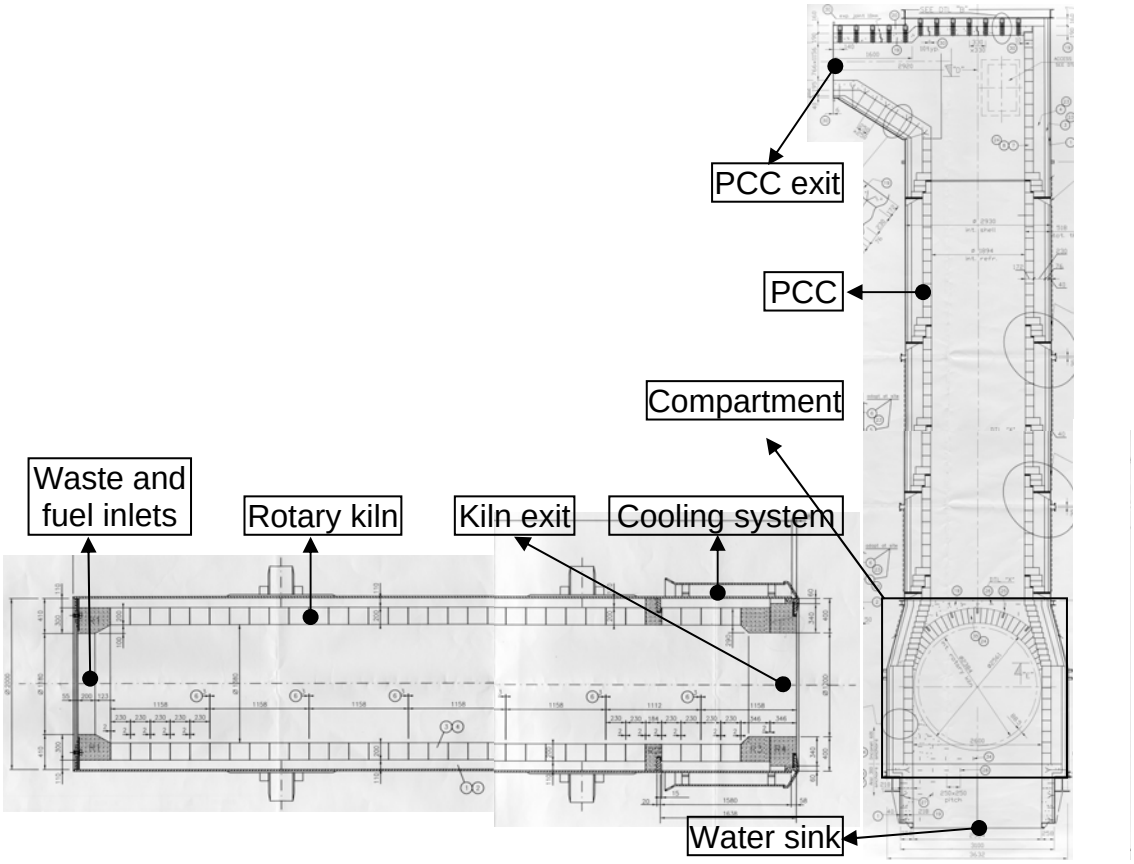

Figure 1.1: Rotary kiln and PCC

An unexpected problem arises while THERESA is running. The ashes, which are composed of softened glass-like materials in high temperature, can stick on the inner surface at the exit. A part of them do not drop down into the water sink and are accumulating gradually at the exit of the rotary kiln, which decreases the inner diameter of the rotary kiln. One of the reasons that the ashes do not exit might be that the compartment temperature is so low that the coagulating process of the ashes into glass-like materials is too fast. One can suspect that the cooling system is too efficient, or that the water evaporation in the water sink affects adversely the temperature distribution in the compartment. A measure to increase the compartment temperature could be installing additional heaters in the compartment walls.

2. Objectives

This work of numerical simulations is carried out to determine the detailed thermal and fluid dynamic fields in the THERESA facility. Especially, three factors, which could influence the gas parameter distributions in the compartment between the rotary kiln and the PCC, are investigated numerically: the influence of different boundary conditions of the compartment walls, the influence of the cooling system at the compartment switched on or off, and the influence of the steam as a cooling source from the water sink.

FLUENT is a commercial computer code for modeling reacting or non-reacting flows and heat transfer processes in complex geometries [1]. FLUENT solves flow problems with structured or unstructured meshes that can be generated for complex geometries. For three-dimensional simulations, meshes with tetrahedral, hexahedral, pyramidal, wedged, and hybrid meshes are provided. Therefore, FLUENT is chosen to simulate numerically the THERESA system.

3. Numerical assumptions

3.1 Rotary kiln and PCC

The wall of the rotary kiln contains three solid layers, being made of different types of materials, which are used as heat insulation and structure support. The inner wall is mainly made out of ALRO 85 F; the external wall is out of steel; the layer in between consists ATLAS. The material CAST 8004 CR is used in some supporting parts. The thermal dynamic properties of these materials are listed in Appendix I.

In order to make the model of the rotary kiln as close as possible to reality, the three solid layers are modeled, besides the reacting flow model in the kiln.

In reality, the wall of the PCC also has multi-layer structure for thermal insulation. However, it is not modeled because of its smaller impact on the interested domain.

3.2 Fuel and oxidant

In THERESA, waste is burnt with natural gas or oil, and air is used as oxidant. The nominal volumetric flow rate of natural gas is about 150 bar m^3/h, which is equivalent to a thermal power of 1.5 MW. In order to simplify the problem, in numerical simulations only methane and air are injected into the rotary kiln, with a mass flow rate of 2.72×10^{-2} kg/s, which corresponds approximately to the power of 1.5 MW.

3.3 Auxiliary systems

- Cooling system
  At the exit of the rotary kiln, the metal structure is cooled by cold air driven by eight nozzles. The total volumetric flow rate of all the eight nozzles is about 750 bar m^3/h with the reference temperature of 25 °C. Each nozzle has a hydraulic diameter of 7.694×10^{-2} m.

- Water sink
  The cooling effect of the water sink is modeled by specifying different steam flows from the surface of the water sink. The specified steam mass flow rates in the calculations are 10^{-6} kg/s, 10^{-2} kg/s, and 10^{-1} kg/s, respectively. The temperature of the water sink is assumed as 100 °C.

4. Geometry and mesh

4.1 Geometry

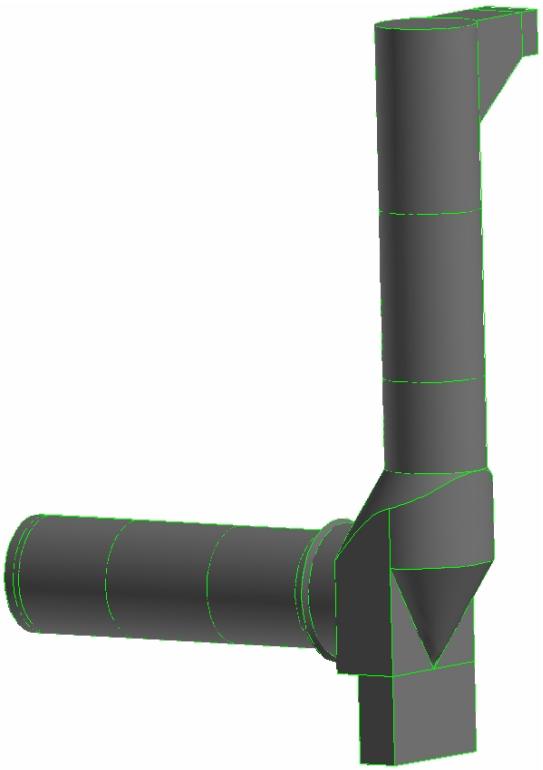

Figure 4.1.1: 3D whole view of THERESA

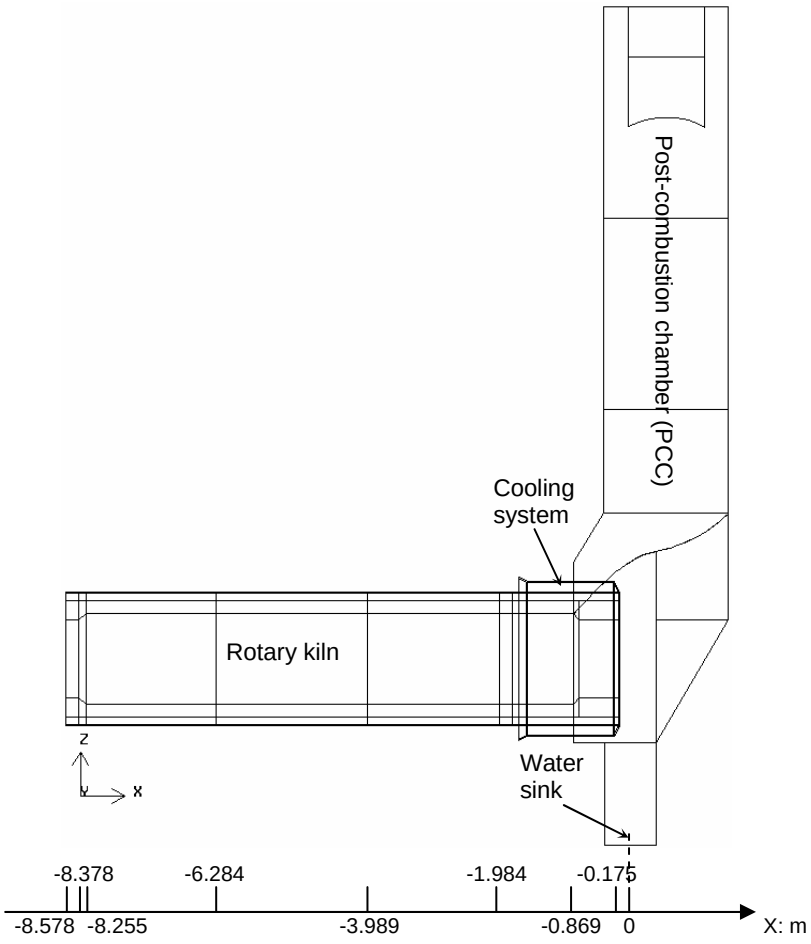

Figure 4.1.2: Complete geometry of THERESA

The total three-dimensional view of THERESA model is shown schematically in Figure 4.1.1, and the complete geometry with some dimensions is shown in Figure 4.1.2.

The geometry contains totally 29 control volumes, 110 independent walls, 61 pairs of coupling walls, and in total 550,000 cells, which supplies a basic impression about the scale of the numerical simulation.

4.2 Meshing strategies

Basically, the solid volumes of the rotary kiln are meshed with a regular, structured grid of hexahedral mesh elements, and all the gas volumes in the whole geometry, except the volume of the compartment, are meshed with wedge elements by using the “Cooper” tool in GAMBIT [2]. The compartment volume is meshed with tetrahedral/hybrid mesh elements because of its irregular geometrical form. As examples, the mesh of the whole geometry is presented in Figure 4.2.1, the meshes of the left end and middle sections of the rotary kiln are shown in Figure 4.2.2 and Figure 4.2.3, respectively, and the mesh of the compartment volume is shown in Figure 4.2.4.

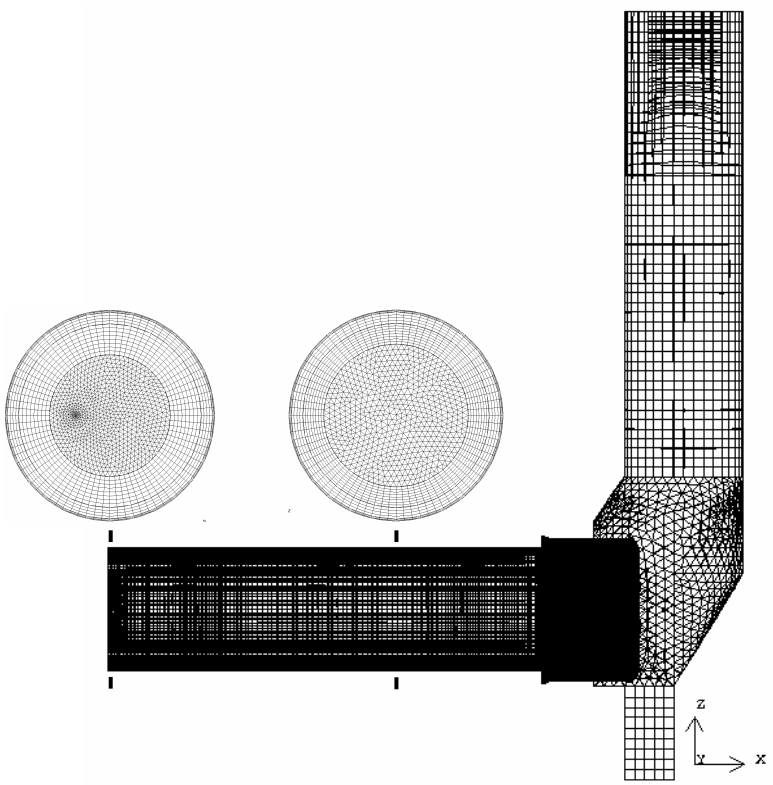

Figure 4.2.1: Mesh of the whole geometry

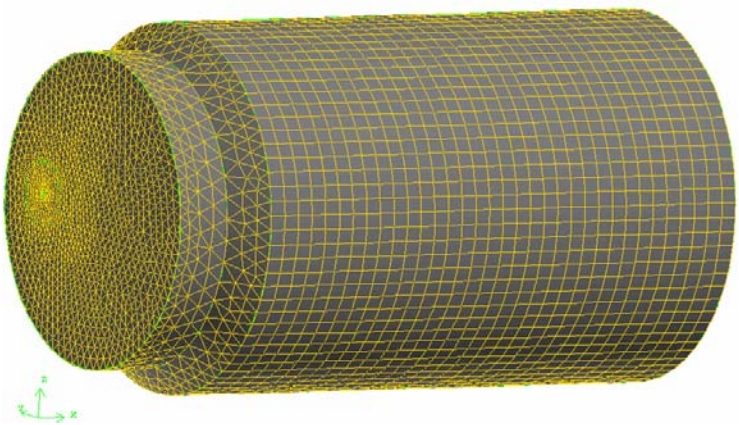

Figure 4.2.2: Mesh of gas volumes at left end of the rotary kiln

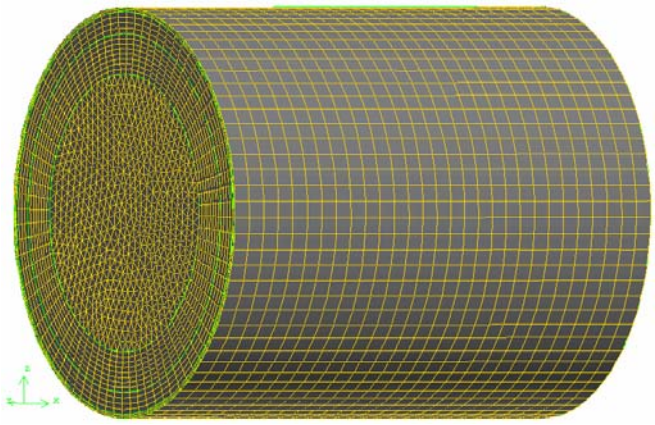

Figure 4.2.3: Mesh of middle section of the rotary kiln including the gas volume and the solid volumes

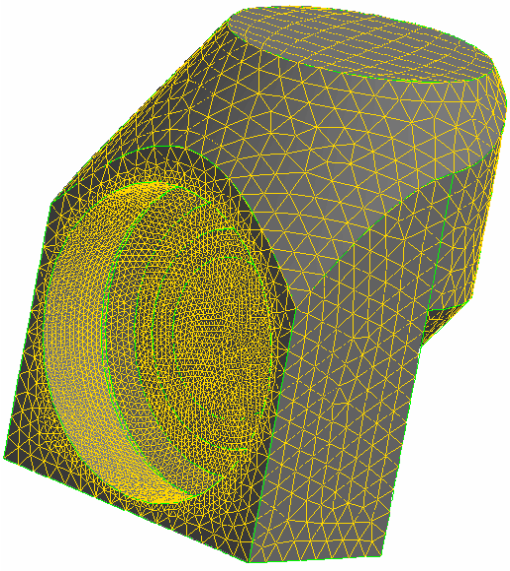

Figure 4.2.4: Mesh of the compartment volume

As depicted in Figure 4.2.1, the mesh in the rotary kiln volumes is denser than that in the PCC, because the flow field in the rotary kiln is of larger interests than in the PCC. (However, the compartment volume in the PCC is of great interest in this simulation). Figure 4.2.2 shows that more refined meshes are used in the zone of the fuel jet, in which the flow could change considerably in very tiny dimensions because of the high velocity of injection. Turbulences are very prominent in this zone.

Five different versions of mesh schemes are applied and summarized in Table 4.2.

- Both a coarse mesh consisting of about 228,000 cells and a refined mesh with more than 1 million cells are set up.

- In one scheme, a coarser mesh is used in general parts, and a more refined mesh in some important domains such as the fuel jet zone, and the zones in which the flow field changes largely, such as the compartment volume. On the other hand, a grid with uniform cell size in all domains is also tested.

- A mixing mesh with both structured grid and unstructured grid is applied, and a totally tetrahedral mesh (unstructured) is adopted too.

Table 4.2: Mesh data used in different versions

Items	Mesh 1	Mesh 2	Mesh 3	Mesh 4	Mesh 5
Layer No. of cell in steel	2	2	2	2	2
Layer No. of cell in ATLAS	3	4	4	4	4
Layer No. of cell in ALRO	4	8	8	8	8
Grid interval in rotary kiln	0.1	0.08	0.08	0.075	0.07
Grid interval in cooling system	0.07	0.05	0.07	0.06	0.05
Grid interval in PCC	0.2	0.1	0.15	0.15	0.14
Cell No. in rotary kiln	185,395	752,814	464,987	549,841	667,724
Cell No. in PCC	43,363	323,666	81,619	90,398	112,512
Total cell No.	228,758	1,076,480	546,606	640,239	780,236

Smoothing and face swapping are tools that complement mesh adaptation, usually increasing the quality of the final numerical mesh [1]. In the application, the techniques are adopted to improve the mesh quality.

5. Boundary conditions

5.1 Fuel and air inlets

A simplified geometry of the fuel/air jet of THERESA is shown in Figure 5.1.1.

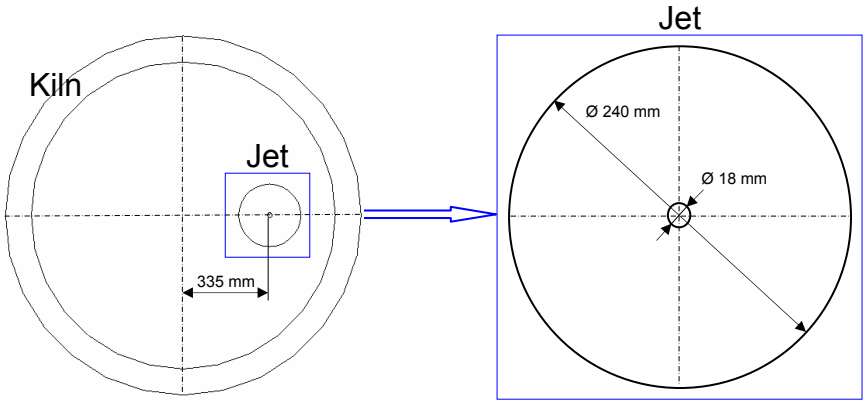

Figure 5.1.1: Geometry of fuel and air injection

Methane is injected from the small pipe in the center of the jet with a mass flow rate of 2.72×10^{-2} kg/s; air is injected from the annular space of the jet with a mass flow rate of 0.6877 kg/s. They are injected in the same direction, however, not along the axis of the rotary kiln but in a direction with a deviation of 6°. While specifying boundary condition in FLUENT, it is necessary to know some geometrical parameters, which can be easily calculated. The cross section of the methane inlet is 2.545×10^{-4} m^2 with a hydraulic diameter of 1.8×10^{-2} m; and the cross section of the air inlet is 4.498×10^{-2} m^2 with a hydraulic diameter of 0.222 m.

5.2 Pressure outlet

The parameter configurations of the back flow at the pressure outlet are important, to some extent, in respect to numerical stability. In reality the back flow should be cold air. However, it will facilitate to get stable calculations if the fluid of back flow is configured to be similar to the fluid in the controlled domain right before the outlet.

5.3 Porous jump boundary condition

In principle porous jump conditions are used to model a thin “membrane” that has known velocity/pressure drop characteristics. It is essentially a 1D simplification of the porous media model available for cell zones. However, in numerical applications, this model is used whenever possible because it is more robust and yields much better convergence [1].

5.4 Wall boundaries

The external walls are specified as external radiation boundary condition with room temperature as the external temperature. Simulation results show that this boundary condition is corresponding to the external walls having fixed temperature of 300 °C.

6. Models

- Turbulence
  Both the standard k-epsilon two-equation model and the RNG k-epsilon turbulence model are tested.

- Near wall treatment
  Both the standard wall function and the enhanced wall treatment function are applied.

- Continuity
  Compressible ideal gas model is selected.

- Energy
  For a detailed analysis, the radiation effect in the model is considered in the THERESA simulations. Additionally, in FLUENT configurations, there is an energy source term of species diffusion in the energy equation, which can be selected or deselected. This option could influence numerical stability.

- Chemistry
  One step of global reaction between methane and oxygen is adopted in chemical modeling,

  $CH_4 + 2\ O_2 \leftrightarrow CO_2 + 2\ H_2O$.

  In this application, turbulent mixing is the main factor affecting the overall chemical reaction rate. Therefore, the eddy-

dissipation model is applied to simulate the turbulence-chemistry interaction.

7. Solution strategies

7.1 Solvers

FLUENT supplies two sorts of solvers. The one is the so called segregated solver, which solves the governing equations sequentially; the other is the coupled solver, in which the governing equations are solved simultaneously. Both the segregated implicit solver and the coupled implicit solver are applied.

Appendix II presents summaries produced by FLUENT on mesh, materials, models, solution controls and others. Appendix III shows the process of problem setup in FLUENT.

7.2 Initial guess

An example for an initial guess is given in Table 7.2, beginning with hot burning products of methane-air mixture in the domain. The table reproduces the computational result of the STANJAN program, a computer code developed by William Reynolds in Stanford University for determining the equilibrium states of combusted gases [3].

Table 7.2: Example for initial guess

Species	O_2	N_2	CO_2	H_2O
Mass fraction	0.1132	0.7452	0.07784	0.06373
Temperature, K	1482			

7.3 Solution controls

The default large under-relaxation factors could be too aggressive to get convergence for a segregated solver. So, in the early calculation, a setting of small under-relaxation factors can be used. They can be increased gradually as the calculation proceeds. Similarly, the coupled solver normally begins with small Courant number, which can be increased step by step afterwards.

It should be emphasized that in THERESA simulations, a smaller momentum under-relaxation factor, instead of default value of 0.7, and

a smaller energy under-relaxation factor, instead of default 1.0, will facilitate to get much lower residuals (readily faster to convergence).

7.4 Discretization

Different discretization schemes like first order upwind scheme, second order upwind scheme and so-called QUICK scheme are tested. The first order scheme makes it easier to converge. However, the second order scheme makes solutions more accurate.

7.5 Solution steps

In the complex reacting flow simulations for THERESA, some important solution steps are followed:

- The non-reactive flow is calculated for starting. Then the chemistry model is activated.

- The isothermal flow calculation can proceed first. Then the energy equation is activated.

- The calculation can proceed without the turbulence model. Then the turbulence model is turned on.

7.6 Mesh adaptations

A salient feature of FLUENT is that one can adapt the mesh based on the obtained solution [1]. It is possible to refine or coarsen the mesh. Adaptations can make the calculation more stable or the solution more accurate. For examples,

- To refine the mesh based on temperature and/or its gradient, or based on species mass fraction of methane and/or its gradient.

- To refine certain volumes defined geometrically, e.g., the zone of the fuel jet.

In THERESA calculations, the grids of cylindrical volumes containing the major part of the jet flame are refined sequentially. The cylinders are defined in Table 7.6. Point 1 is the center of one end of the cylinder; point 2 is the center of the other end.

Table 7.6: Geometrical definition of cylinders for grid adaptation

Cylinder		1st		2nd		3rd	
Point		1	2	1	2	1	2
Coordinate, m	X	-8.678	-8.078	-8.678	-7.978	-8.678	-7.878
	Y	0.34617	0.27917	0.34617	0.268	0.34617	0.25683
	Z	2.838	2.838	2.838	2.838	2.838	2.838
Radius, m		0.13		0.14		0.15	

7.7 Judge convergence

Normally, it is enough to monitor the residuals to judge whether the solution is converged or not. However, this could mislead in some cases, e.g. when the initial guess is too good and is very close to the real solution. Therefore, it is quite necessary to monitor simultaneously coefficients of drag, moment or heat transfer on critical walls, and some integrated quantities in critical volumes. In THERESA simulations, the way to make animations about the parameter distributions of flow fields is also adopted for the convergence judgment.

8. Results

As an example, one simulation result is presented in this section. The third version of mesh in Table 4.2 is adopted, which is the hybrid mesh including both structured and unstructured cells. The total cell number is 546,606.

Some important boundary condition specifications are listed here:
- the compartment walls have external radiation boundary condition,
- the cooling system is activated,
- the steam mass flow rate from the water sink is 10^{-6} kg/s.

The principle models being used are:
- standard k-epsilon two-equation turbulence model,
- discrete ordinate (DO) radiation model,
- eddy-dissipation chemistry-turbulence interaction model,
- compressible ideal gas model, and
- standard wall functions.

In this simulation, the three-dimensional segregated implicit solver is used to search the solution. The computational results for the

temperature, the flow field, the turbulence and the species distributions are shown in the following sections.

8.1 Temperature distributions

The temperature distributions in a vertical plane and a horizontal plane, which cut through the axis of the rotary kiln, are shown in Figure 8.1.1 and Figure 8.1.2, respectively. According to the figures, the length of the combustion zone, or the flame length, is about one third of the whole length of the rotary kiln of 8.4 m. The flame is asymmetric because the jet position is not on the rotary kiln axis and the injection is not along the direction of the axis.

The temperature distributions in planes perpendicular to the rotary kiln axis are shown in Figure 8.1.3 for different x-coordinates, which shares the same color index as Figure 8.1.1. The relation between the positions and x-coordinates refer to Figure 4.1.2. The series of figures record the development of the flame in the direction of x-coordinate.

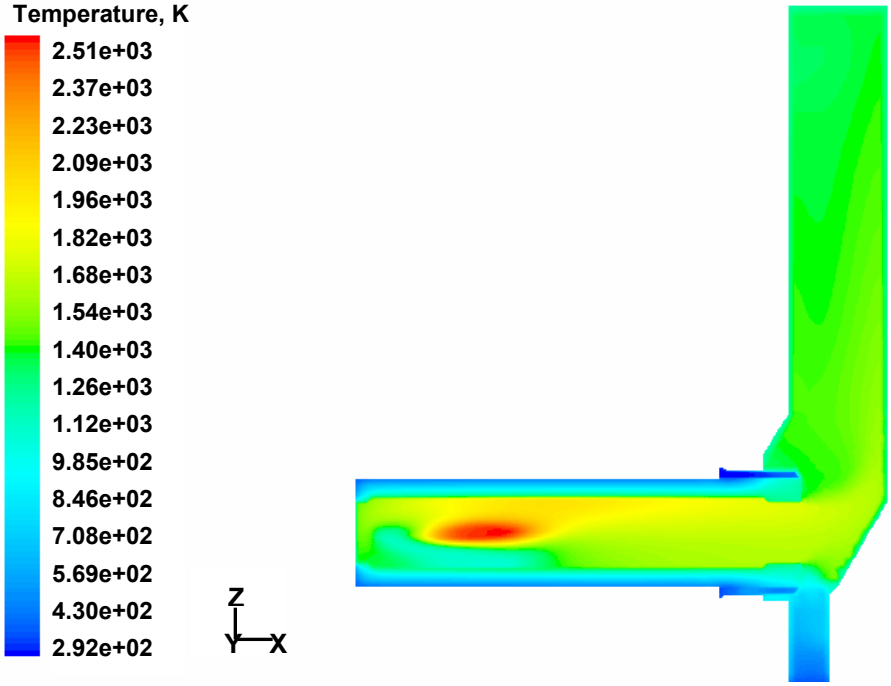

Figure 8.1.1: Temperature distribution in vertical plane through axis of rotary kiln

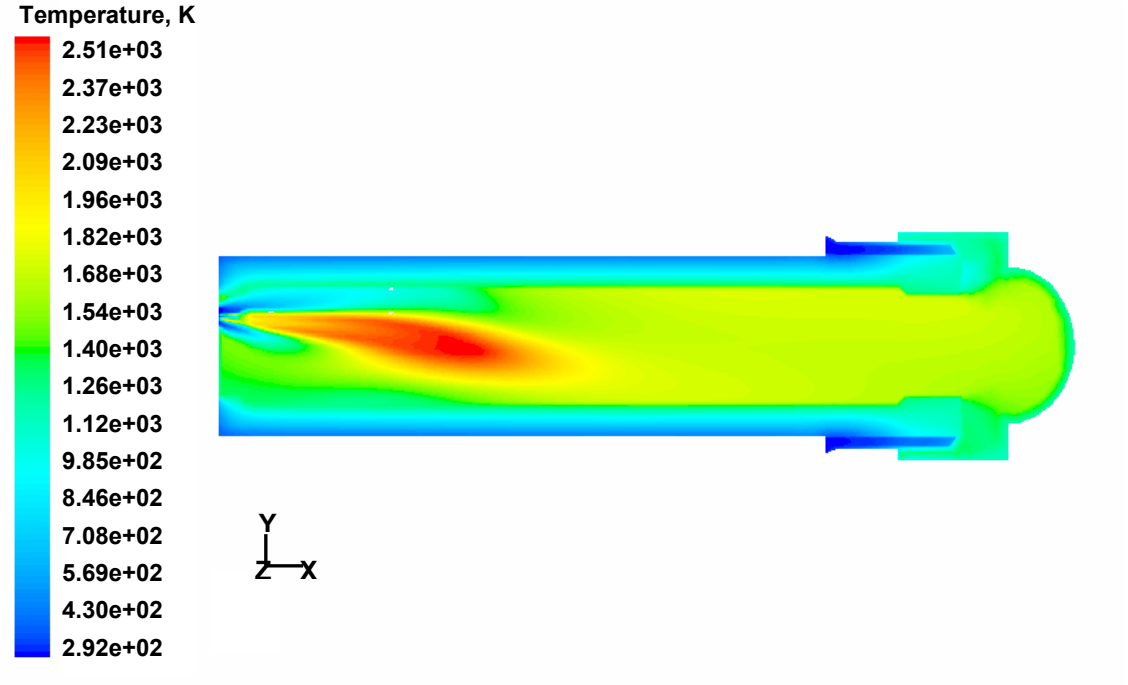

Figure 8.1.2: Temperature distribution in horizontal plane through axis of rotary kiln

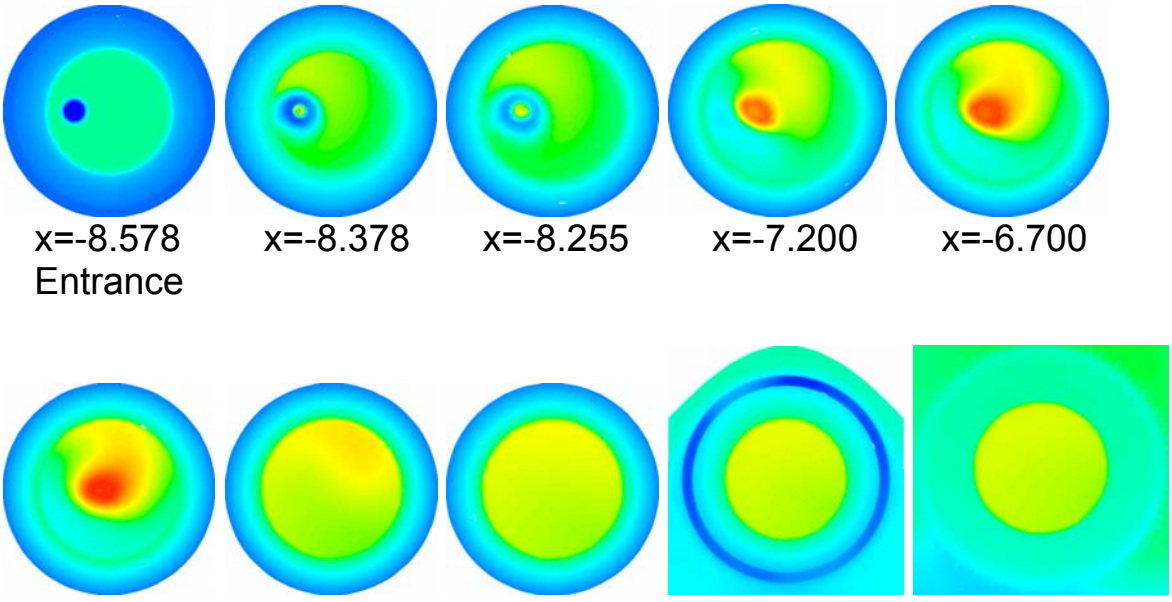

Figure 8.1.3: Temperature distributions at different x-coordinates

Some important temperature information is listed as follows:

- the maximal temperature of flame is about 2603 K,
- the average gas volume temperature of the rotary kiln is about 1661 K,
- the average gas volume temperature of the PCC is about 1375 K,
- the average gas volume temperature of the compartment is about 1428 K,
- the average gas temperature at the exit of rotary kiln is about 1709 K.

A more detailed temperature distribution in the compartment domain is presented in Figure 8.1.4, with a color index different from that of Figure 8.1.1. As seen from the figure, the temperature of the gas volume right above the water sink is quite low, in average 625 K, although a tiny water evaporation rate of 10^{-6} kg/s is assumed. Of course, the cooling system also makes a contribution to cool down the wall of the rotary kiln.

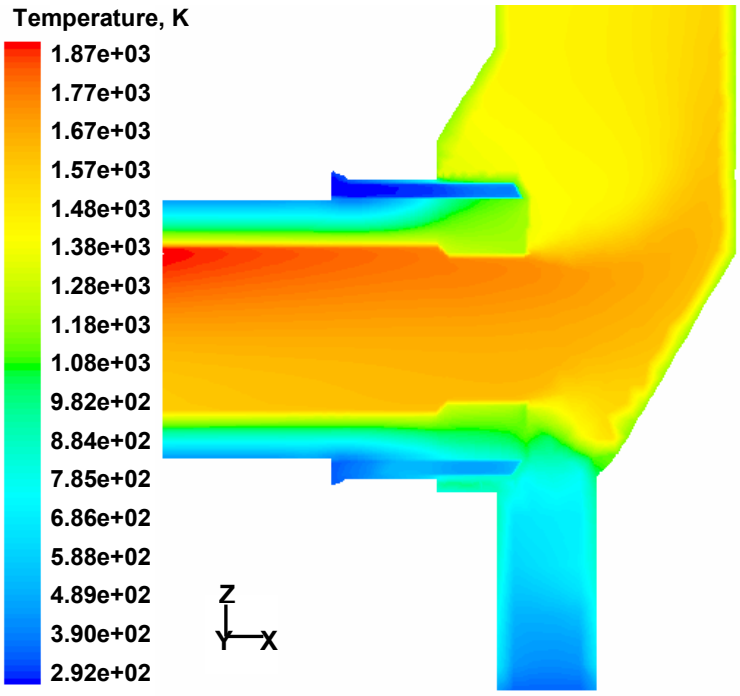

Figure 8.1.4: Temperature distribution in the compartment

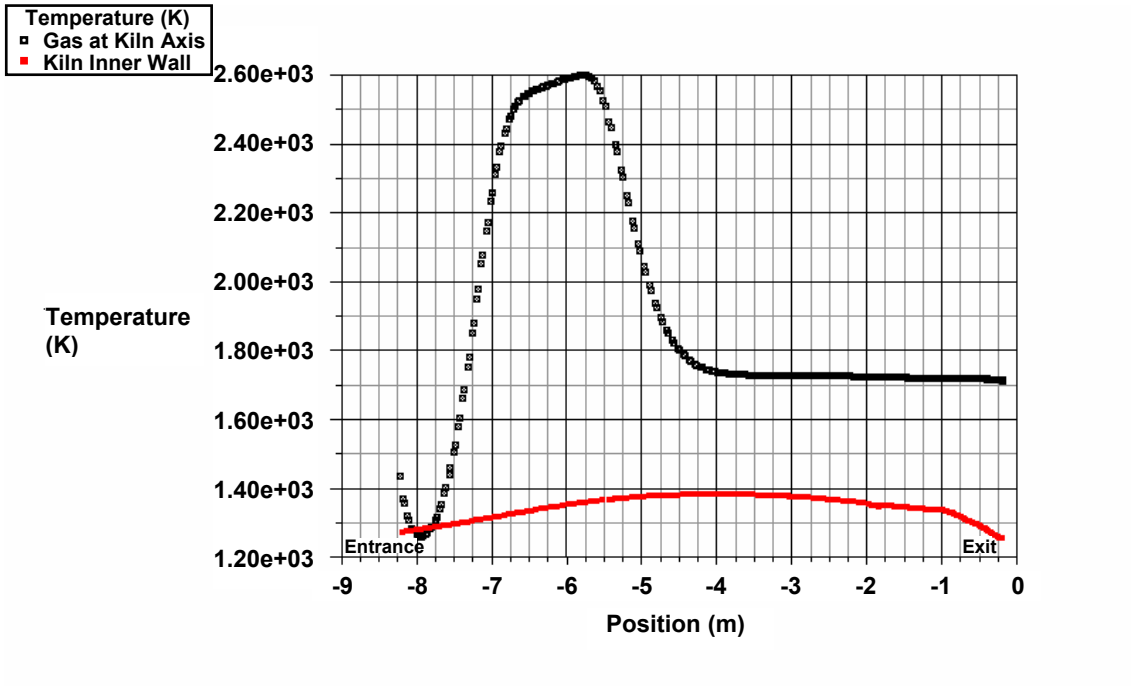

Figure 8.1.5: Temperature profiles of gas and wall

The gas temperature profiles along the axis and at the solid inner wall are shown in Figure 8.1.5. From the gas temperature profiles, it can be concluded that the gas temperature drops just slightly in the zone of post-combustion between -4 m and -0.175 m in x-coordinate. However, the inner wall temperature decreases dramatically by about 130 K in this zone. This is caused by the heat loss by the thermal radiation from the external walls of the rotary kiln, and certainly also by the cooling effect of the cooling system. It is interesting, that the temperature descends the fastest in the area right close to the exit. This is because the kiln section between -0.869 m and -0.175 m is contained in the compartment volume (referring to Figure 4.1.2), and the gas temperature in this zone is relatively lower than that of other zones in the compartment volume, which can be seen from Figure 8.1.4.

One can imagine that if the total length of the rotary kiln were shorter, or if the length of the kiln section containing in the compartment volume were shorter, the inner wall temperature of the rotary kiln would be higher. Then, the glass-like molten ashes sticking around the exit might be wiped away owing to the higher temperature.

8.2 Flow field distributions

The flow field in the zone of the fuel jet is shown in Figure 8.2.1. The highest velocity of the jet is about 185 m/s. The tiny dimension (0.018 m) of the jet elevates the jet velocity when mass flow rate is given. Such a high velocity and the asymmetry of the injection make the complexity of the jet flow in the zone. As seen from the figure, there are big eddies formed by the back flows around the fast jet flow in the center. The flow field in the compartment zone is shown in Figure 8.2.2, which shows that the main flow is bent by the compartment walls opposite to the exit of the rotary kiln. The change of the flow direction results in vortices both on the top and bottom of the main flow. The average velocity at the exit of the kiln is about 3.2 m/s.

8.3 Turbulence

The standard k-epsilon two equations turbulence model is adopted in the simulation. The distributions of turbulence kinetic energy and dissipation rate are shown in Figure 8.3.1 and Figure 8.3.2, which show that turbulence occurs mainly in the combustion zone.

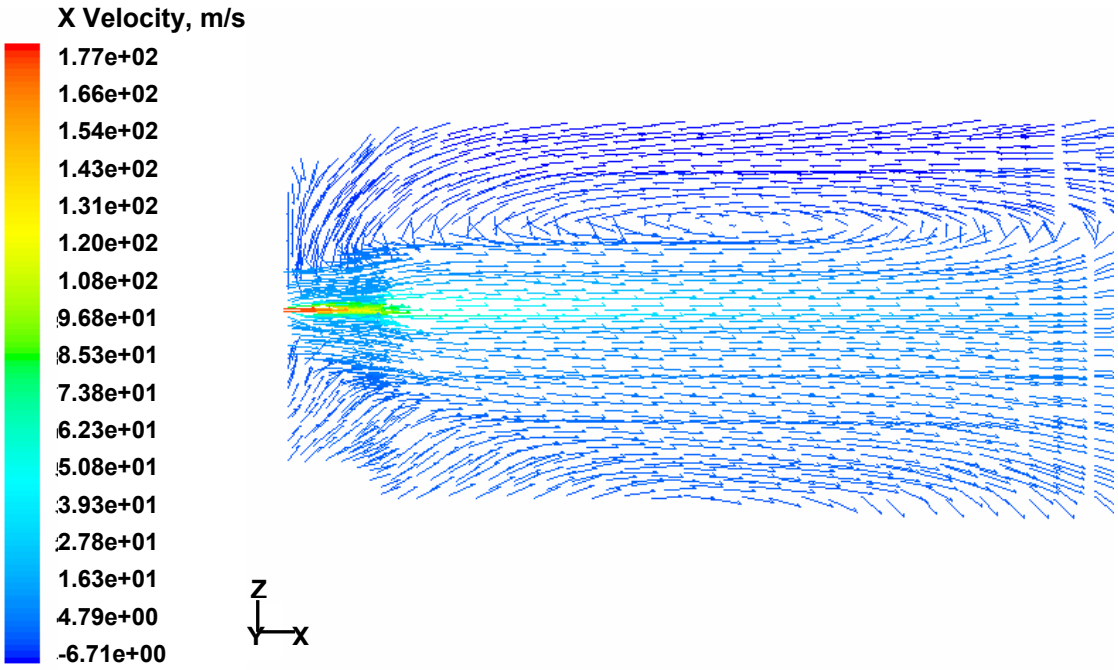

Figure 8.2.1: Flow field in jet zone

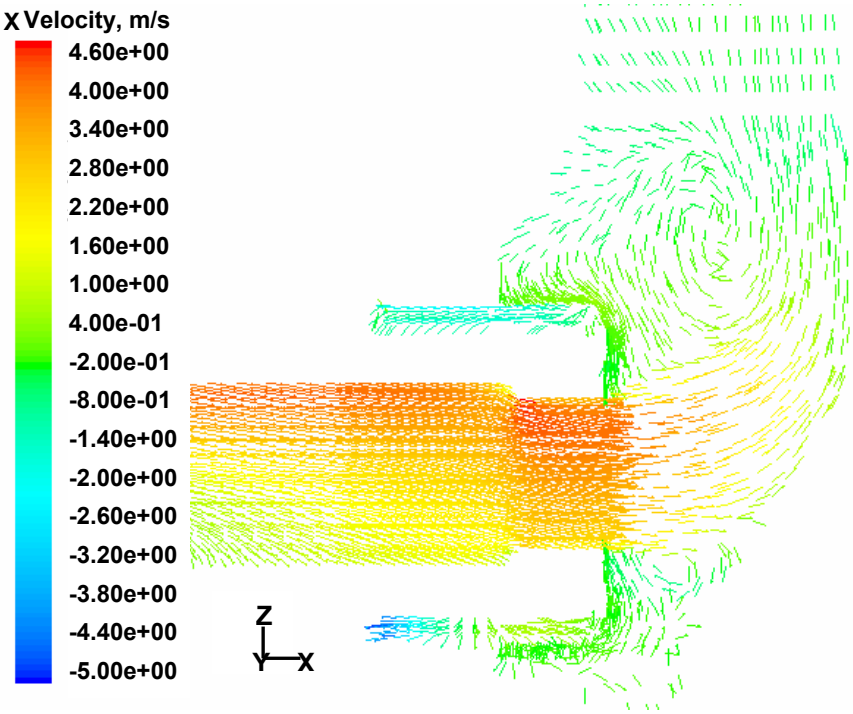

Figure 8.2.2: Flow field in the compartment

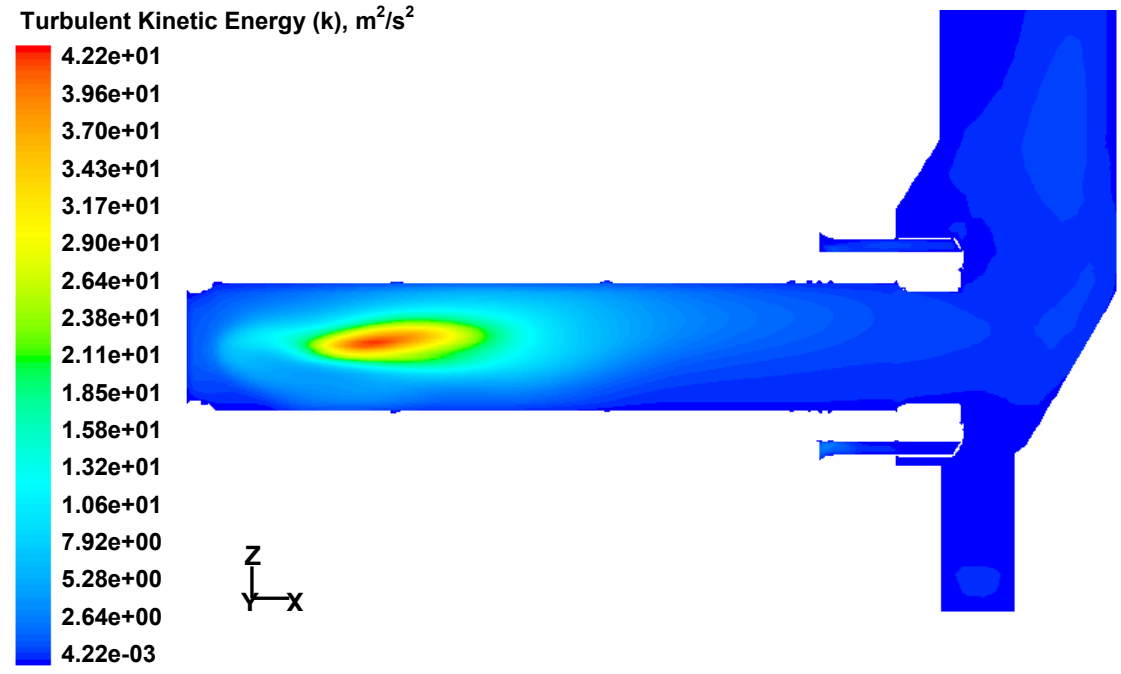

Figure 8.3.1: Turbulence kinetic energy distribution

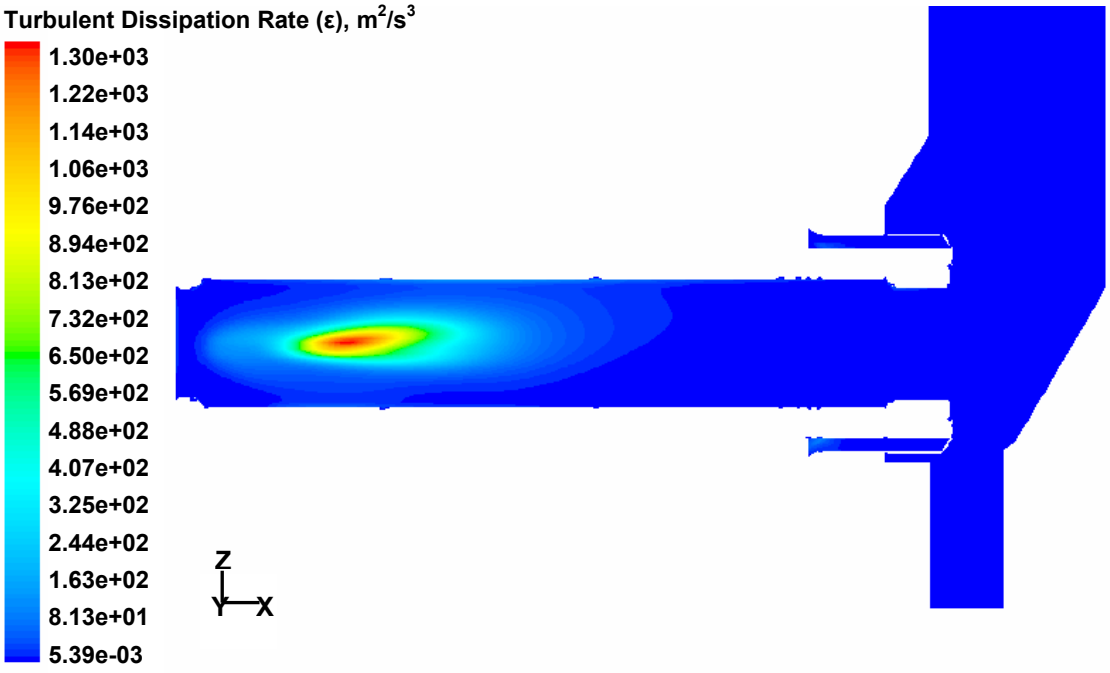

Figure 8.3.2: Turbulence dissipation rate distribution

8.4 Species

The mass fraction distributions of fuel and oxidant are shown in Figure 8.4.1 and 8.4.2. According to the figures, the methane/oxygen combustion takes place very fast and methane is consumed swiftly, therefore, the methane profile appears only in a tiny region. The oxygen distribution represents the flame shape. In the compartment zone, the red color is representative of the oxygen in the ventilating air of the cooling system, which is separated from the methane/air combustion system. The distributions of burned products, CO_2 and H_2O, are shown in Figure 8.4.3 and 8.4.4. The contours of flame are reproduced in the figures. The products are generated mainly in the combustion region and then diffuse in the combustion chamber.

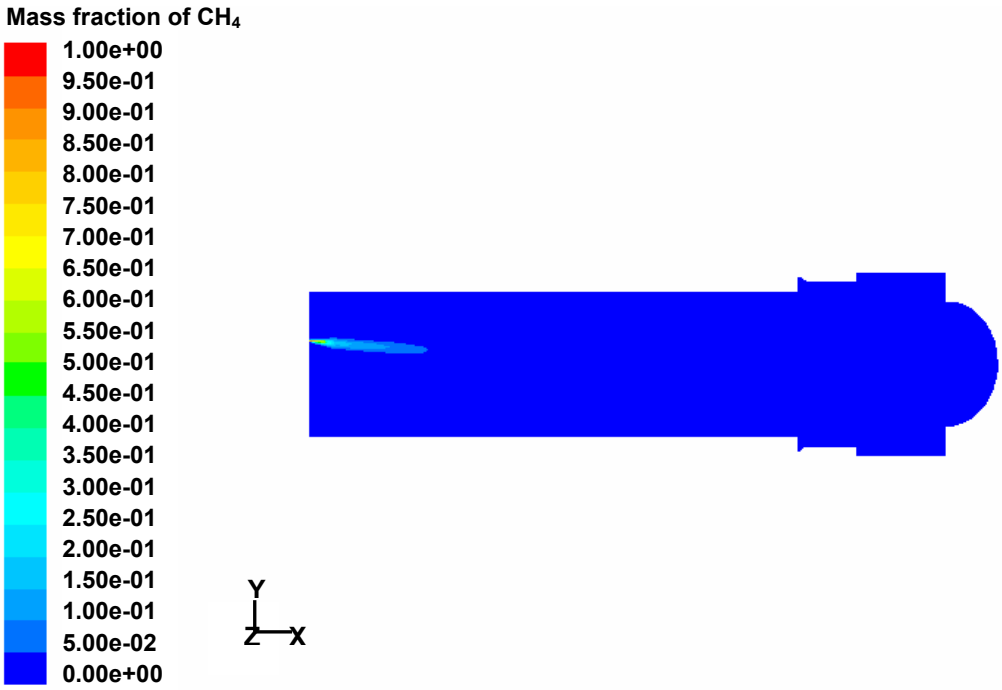

Figure 8.4.1: Mass fraction distribution of CH_4 in rotary kiln

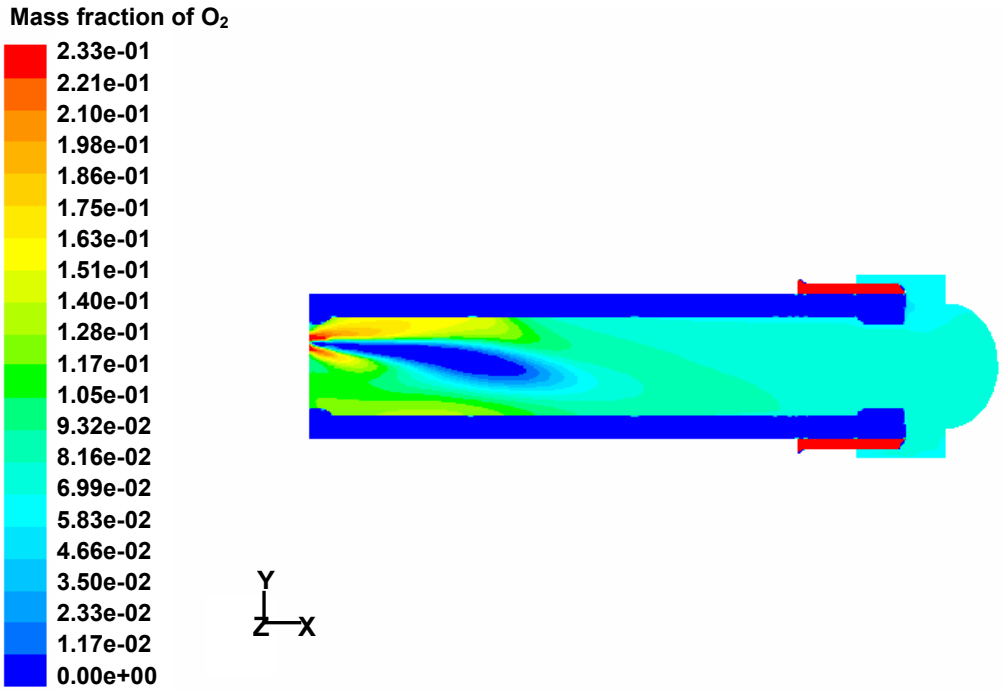

Figure 8.4.2: Mass fraction distribution of O_2 in rotary kiln

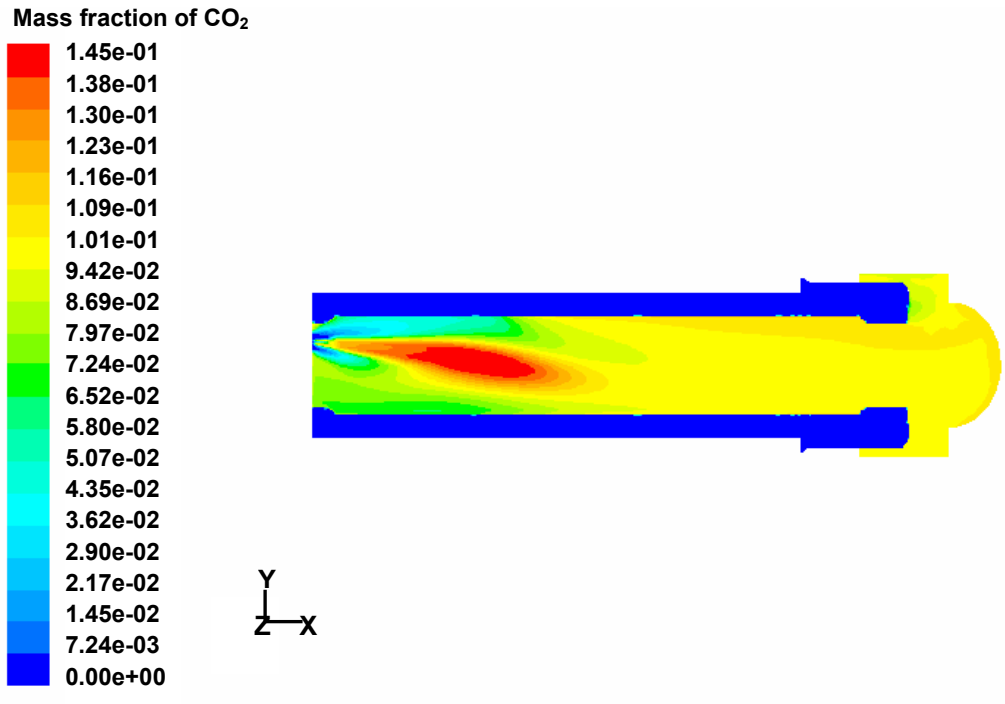

Figure 8.4.3: Mass fraction distribution of CO_2 in rotary kiln

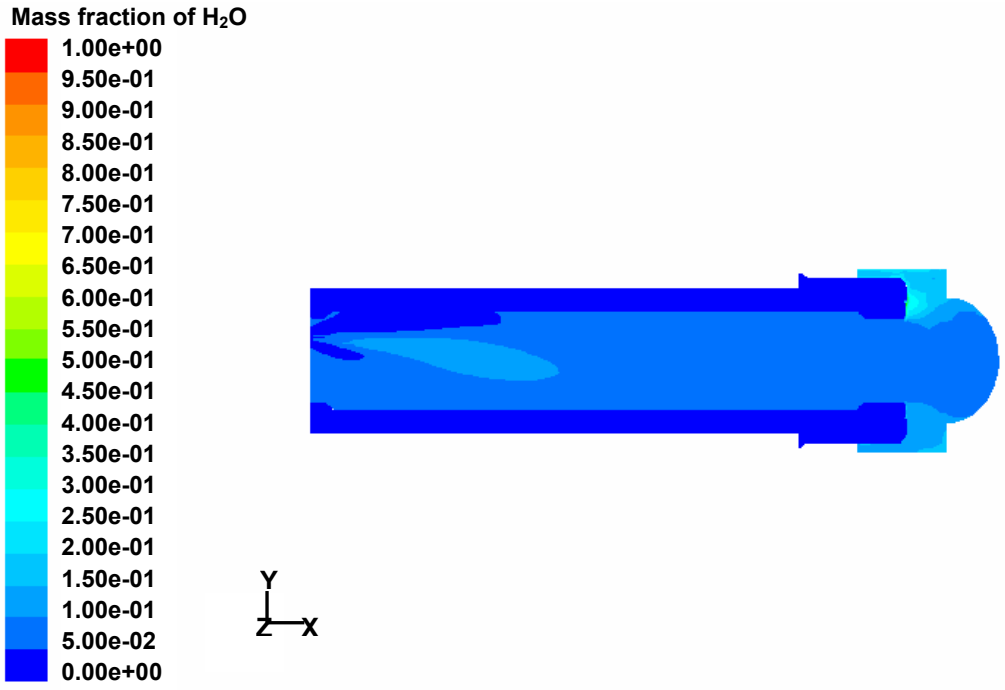

Figure 8.4.4: Mass fraction distribution of H_2O in rotary kiln

9. Analyses

The compartment between the rotary kiln and the PCC is of great interest because the ashes always accumulate at the exit of the rotary kiln. Therefore, the influences of three sources, which could play a key role on the temperature distribution at the exit of the rotary kiln, were assessed:

- the influence of the radiation feedback from the PCC walls,
- the influence of cooling system protecting the steel envelope at the exit of the rotary kiln, and
- the influence of steam as a cooling source coming from the water sink below the exit of the rotary kiln.

To study the radiation feedback, the temperature of the compartment walls was fixed at 800 K, 1000 K, 1200 K, and 1400 K, and influence on the axial temperature of the rotary kiln was investigated. The calculation results did not exhibit noticeable difference compared to that obtained by using the radiation boundary condition. The results of the different cases are summarized in Table 9.1.

Table 9.1: Influence of fixed temperature boundary of the compartment walls† on the combustion

Fixed temperature, K	Heat flux through the walls, W	Axial temperature at exit of rotary kiln, K
800	-10540	1695.4 ± 6.3
1000	-4789	1696.6 ± 5.8
1200	732	1702.3 ± 9.0
1400	6505	1704.6 ± 9.0
Radiation B. C.	-21135	1695.1 ± 6.3

† Only the walls, which are right opposite to the exit of the rotary kiln, have fixed temperature. The four walls are colored in Figure 9.1, to distinguish them from those with radiation boundary condition.

The influence of the cooling system was studied by injection of cold air into the annular space of the wrapper. At the axis of the rotary kiln the observed temperature difference between the cases with activated and deactivated cooling system did not exceed 11 K.

The cooling effect of the steam from the water sink was modeled by specifying different steam flows from the water surface. Three cases were considered with total steam flow rates equal to 10^{-6} kg/s, 10^{-2} kg/s and 10^{-1} kg/s, respectively. The third case is obviously is beyond normal operating conditions and was included in the parameters set to cover the widest range of possible conditions. For these three cases the maximum differences between observed axial temperatures achieved the following values: 0 K, -5.1 K, and -23.1 K.

The computational results about different cooling conditions and different water evaporations are summarized in Table 9.2.

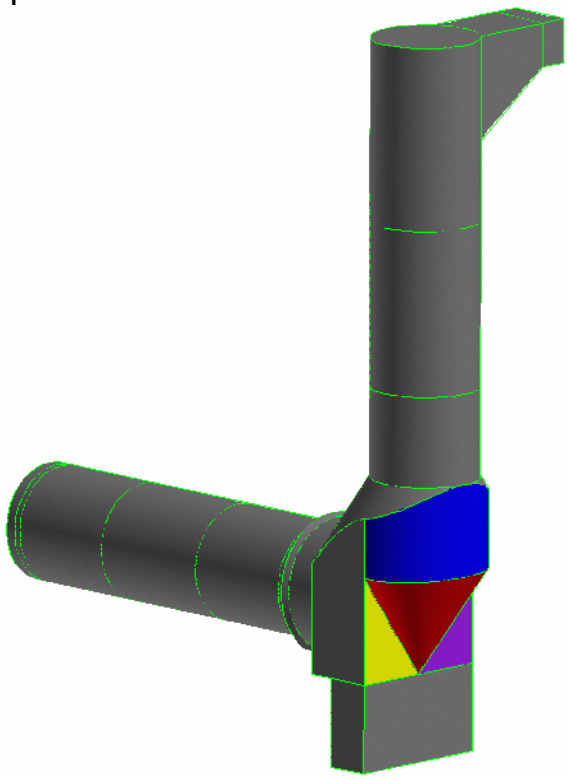

Figure 9.1: Compartment Walls with fixed temperature

Table 9.2: Influences of cooling system and water evaporation on the combustion

Case	Configurations		Axial temperature at exit of rotary kiln, K	Temperature difference comparing to Case 1, K
	Cooling system	Water evaporation, kg/s		
1	on	10^{-6}	1695.1 ± 6.3	0
2	on	10^{-2}	1690.0 ± 2.0	-5.1
3	on	10^{-1}	1672.0 ± 2.0	-23.1
4	off	10^{-6}	1705.5 ± 8.0	10.4

10. Conclusions

The thermal fluid dynamics and the combustion occurring in THERESA facility have been simulated numerically by using the FLUENT computer code. Physically reasonable distributions of the gas parameters have been obtained by simulations. It is concluded that the combustion takes place essentially in the first half of the kiln, and that, in the second half, the wall temperature decreases because of thermal radiation to the atmosphere. It was investigated whether this situation is influenced significantly by (i) the cooling system, (ii) the water evaporation from the water sink and (iii) the thermal radiation of the compartment walls. Numerical simulations indicate that the considered phenomena influence to some extent the temperature at the exit of the rotary kiln, but do not play key roles. Measures to avoid too low temperatures at the kiln exit could be (i) making shorter the whole length of the rotary kiln, or (ii) installing the injection at a position more downstream if the first solution is not feasible, (iii) shortening the kiln section in the compartment volume and/or (iv) thermally insulating it better from the relatively cold volume in the compartment.

Acknowledgements

Many thanks to Dr. J. Starflinger for his good advices to revise this report. The authors also do appreciate Dr. K. H. Scholl in ITC-TAB for his supply of useful information about THERESA and many insights on this problem.

References

[1] FLUENT 6.0 Documentation, Fluent Inc., 2001
[2] GAMBIT User's Guide, Fluent Inc., 2000
[3] Reynolds, W.C., 1986, The Element Potential Method for Chemical Equilibrium Analysis: Implementation in the Interactive Program STANJAN, Stanford University Press, ME 270, no.7, 1986

Appendix I

Material Thermal Dynamic Properties

--- Based on JANAF Thermo-Chemical Tables (3rd Edition, 1996)

- Material: ALRO 85 F, reference temperature 800 K.

Components	Molecule Weight, kg/mol	C_p, J/mol/K	C_p, J/kg/K	Weight Fraction
Al_2O_3	0.10196128	120.135	178.2414	84.5
TiO_2	0.0798788	73.078	914.86101	0.3
Fe_2O_3	0.1596922	158.218	990.76849	0.5
SiO_2	0.0600843	73.701	1226.6266	7.2
CaO	0.0560794	52.40	934.38945	0.1
MgO	0.0403044	49.74	1234.1084	0.1
Na_2O	0.06197894	91.291	1472.9358	0.25
K_2O	0.0941960	105.395	1118.8904	0.25
Cr_2O_3	0.1519902	124.29	817.75009	4.6
$(P_2O_5)_2$	0.28388904	396.643	1397.1762	2.0
Other			1128.6	0.2
Average C_p, J/kg/K			1168.1	
Thermal Conductivity, W/(mK)			1.35	
Density, kg/m^3			3100	

- Material: ATLAS + A, reference temperature 600 K.

Components	Molecule Weight, kg/mol	C_p, J/mol/K	C_p, J/kg/K	Weight Fraction
Al_2O_3	0.10196128	112.545	1103.8014	43
SiO_2	0.0600843	64.417	1072.1104	53
Fe_2O_3	0.1596922	141.168	884.0006	2.2
CaO	0.0560794	50.48	900.15228	0.3
MgO	0.0403044	47.43	1176.7946	0.6
Alkalis		73.942	1208.4648	0.7
Other			1057.6	0.2
Average Cp, J/kg/K			1082.6	
Thermal Conductivity, W/(mK)			1.3	
Density, kg/m^3			2100	

- Material: CAST 8004 CR, reference temperature 800 K.

Components	Molecule Weight, kg/mol	C_p, J/mol/K	C_p, J/kg/K	Weight Fraction
Al_2O_3	0.10196128	120.135	178.2414	87.2
Cr_2O_3	0.1519902	124.29	817.75009	9.5
SiO_2	0.0600843	73.701	1226.6266	2.5
Fe_2O_3	0.1596922	158.218	990.76849	0.1
CaO	0.0560794	52.40	934.38945	0.5
MgO	0.0403044	49.74	1234.1084	0.1
Alkalis		98.343	1295.9131	0.1
Average Cp, J/kg/K			1144.0	
Thermal Conductivity, W/(mK)			2.3	
Density, kg/m^3			3200	

Appendix II

FLUENT Report on Grid

```
Grid Size

Level    Cells    Faces    Nodes   Partitions
    0   503056  1395106   394733            6

 54 cell zones, 298 face zones.
```

FLUENT Report on Materials

```
Material Properties
-------------------

   Material: alro85f (solid)

      Property                     Units    Method      Value(s)
      ------------------------------------------------------------
      Density                      kg/m3    constant    3100
      Cp (Specific Heat)           j/kg-k   constant    1168.1
      Thermal Conductivity         w/m-k    constant    1.35
      Absorption Coefficient       1/m      constant    0.0099999998
      Scattering Coefficient       1/m      constant    0
      Scattering Phase Function             isotropic   #f
      Refractive Index                      constant    1

   Material: water-vapor (fluid)

      Property                     Units       Method     Value(s)
      ------------------------------------------------------------------
      Cp (Specific Heat)           j/kg-k      constant   2014
      Thermal Conductivity         w/m-k       constant   0.0261
      Viscosity                    kg/m-s      constant   1.34e-05
      Molecular Weight             kg/kgmol    constant   18.01534
      Standard State Enthalpy      j/kgmol     constant   -2.418379e+08
      Standard State Entropy       j/kgmol-k   constant   188696.44
      Reference Temperature        k           constant   298.15
      L-J Characteristic Length    angstrom    constant   2.605
      L-J Energy Parameter         k           constant   572.4
      Degrees of Freedom                       constant   0

   Material: oxygen (fluid)

      Property                     Units       Method     Value(s)
      ------------------------------------------------------------
      Cp (Specific Heat)           j/kg-k      constant   919.31
      Thermal Conductivity         w/m-k       constant   0.0246
      Viscosity                    kg/m-s      constant   1.919e-05
      Molecular Weight             kg/kgmol    constant   31.9988
      Standard State Enthalpy      j/kgmol     constant   0
      Standard State Entropy       j/kgmol-k   constant   205026.86
      Reference Temperature        k           constant   298.15
      L-J Characteristic Length    angstrom    constant   3.458
      L-J Energy Parameter         k           constant   107.4
      Degrees of Freedom                       constant   0
```

Material: nitrogen (fluid)

Property	Units	Method	Value(s)
Cp (Specific Heat)	j/kg-k	constant	1040.67
Thermal Conductivity	w/m-k	constant	0.0242
Viscosity	kg/m-s	constant	1.663e-05
Molecular Weight	kg/kgmol	constant	28.0134
Standard State Enthalpy	j/kgmol	constant	0
Standard State Entropy	j/kgmol-k	constant	191494.78
Reference Temperature	k	constant	298.15
L-J Characteristic Length	angstrom	constant	3.621
L-J Energy Parameter	k	constant	97.53
Degrees of Freedom		constant	0

Material: mixture-template (mixture)

Property	Units	Method	Value(s)
Mixture Species		names (co2 h2o o2 ch4 n2)	
Reaction		eddy-dissipation	
((reaction-1 ((ch4 1 1 1) (o2 2 1 1)) ((co2 1 1 1) (h2o 2 1 1)) ((n2 0 1)) (stoichiometry 1ch4 + 2o2 --> 1co2 + 2h2o) (arrhenius 1e+15 100 0) (mixing-rate 4 0.5) (use-third-body-efficiencies? #f)))			
Density	kg/m3	ideal-gas	#f
Cp (Specific Heat)	j/kg-k	mixing-law	#f
Thermal Conductivity	w/m-k	mass-weighted-mixing-law	#f
Viscosity	kg/m-s	mass-weighted-mixing-law	#f
Mass Diffusivity	m2/s	constant-dilute-appx	2.88e-05
Absorption Coefficient	1/m	constant	0.01
Scattering Coefficient	1/m	constant	0
Scattering Phase Function		isotropic	#f
Thermal Expansion Coefficient	1/k	constant	0
Refractive Index		constant	1

Material: carbon-dioxide (fluid)

Property	Units	Method	Value(s)
Cp (Specific Heat)	j/kg-k	constant	840.37
Thermal Conductivity	w/m-k	constant	0.0145
Viscosity	kg/m-s	constant	1.37e-05
Molecular Weight	kg/kgmol	constant	44.009949
Standard State Enthalpy	j/kgmol	constant	-3.9353235e+08
Standard State Entropy	j/kgmol-k	constant	213715.88
Reference Temperature	k	constant	298.15
L-J Characteristic Length	angstrom	constant	3.941
L-J Energy Parameter	k	constant	195.2
Degrees of Freedom		constant	0

Material: methane (fluid)

Property	Units	Method	Value(s)

Cp (Specific Heat)	j/kg-k	constant	2222
Thermal Conductivity	w/m-k	constant	0.0332
Viscosity	kg/m-s	constant	1.087e-05
Molecular Weight	kg/kgmol	constant	16.04303
Standard State Enthalpy	j/kgmol	constant	-74895176
Standard State Entropy	j/kgmol-k	constant	186040.09
Reference Temperature	k	constant	298.15
L-J Characteristic Length	angstrom	constant	3.758
L-J Energy Parameter	k	constant	148.6
Degrees of Freedom		constant	0

Material: steel (solid)

Property	Units	Method	Value(s)
Density	kg/m3	constant	8030
Cp (Specific Heat)	j/kg-k	constant	502.48001
Thermal Conductivity	w/m-k	constant	16.27
Absorption Coefficient	1/m	constant	0.0099999998
Scattering Coefficient	1/m	constant	0
Scattering Phase Function		isotropic	#f
Refractive Index		constant	1

Material: atlasa (solid)

Property	Units	Method	Value(s)
Density	kg/m3	constant	2100
Cp (Specific Heat)	j/kg-k	constant	1082.6
Thermal Conductivity	w/m-k	constant	1.3
Absorption Coefficient	1/m	constant	0.0099999998
Scattering Coefficient	1/m	constant	0
Scattering Phase Function		isotropic	#f
Refractive Index		constant	1

Material: cast8004cr (solid)

Property	Units	Method	Value(s)
Density	kg/m3	constant	3200
Cp (Specific Heat)	j/kg-k	constant	1144
Thermal Conductivity	w/m-k	constant	2.3
Absorption Coefficient	1/m	constant	0.0099999998
Scattering Coefficient	1/m	constant	0
Scattering Phase Function		isotropic	#f
Refractive Index		constant	1

FLUENT Report on Models

Models

Model	Settings
Space	3D
Time	Steady
Viscous	Standard k-epsilon turbulence model
Wall Treatment	Standard Wall Functions

Heat Transfer	Enabled
Solidification and Melting	Disabled
Radiation	Discrete Ordinate Model
Species Transport	Reacting (5 species)
Coupled Dispersed Phase	Disabled
Pollutants	Disabled
Soot	Disabled

FLUENT Report on Solution Control

Solver Controls

Equations

Equation	Solved
Flow	yes
Turbulence	yes
Reactions	yes
Discrete Ordinates	yes

Numerics

Numeric	Enabled
Absolute Velocity Formulation	yes

Relaxation

Variable	Relaxation Factor
Turbulence Kinetic Energy	0.8
Turbulence Dissipation Rate	0.8
Turbulent Viscosity	1
Solid	1
Discrete Ordinates	1

Linear Solver

Variable	Solver Type	Termination Criterion	Residual Reduction Tolerance
Flow	F-Cycle	0.1	
Turbulence Kinetic Energy	Flexible	0.1	0.7
Turbulence Dissipation Rate	Flexible	0.1	0.7
Discrete Ordinates	Flexible	0.1	0.7

Discretization Scheme

Variable	Scheme
Flow	Second Order Upwind
Turbulence Kinetic Energy	First Order Upwind
Turbulence Dissipation Rate	First Order Upwind

Time Marching

Parameter	Value
Solver	Implicit
Courant Number	0.1

Solution Limits

Quantity	Limit
Minimum Absolute Pressure	1
Maximum Absolute Pressure	5000000
Minimum Temperature	1
Maximum Temperature	5000
Minimum Turb. Kinetic Energy	1e-14
Minimum Turb. Dissipation Rate	1e-20
Maximum Turb. Viscosity Ratio	100000

Appendix III

Case File Setup for THERESA in FLUENT

The step-by-step operations in FLUENT are listed in this appendix. As an example, some parameter settings especially for THERESA are recorded here.

Step 1. Input mesh

Grid file made by GAMBIT is read into FLUENT. Then check it, and scale and smooth it, if necessary.

Step 2. Model definitions

A solver can be defined in this window.

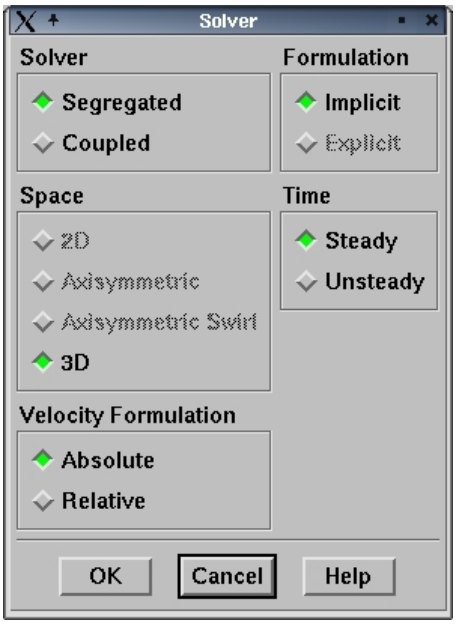

With multiphase model off.

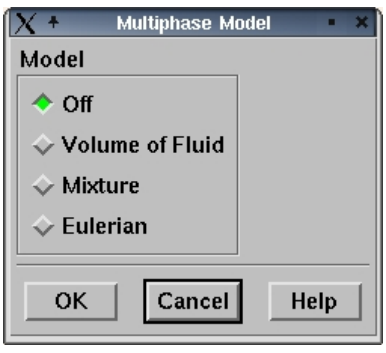

Using this window to define turbulence model.

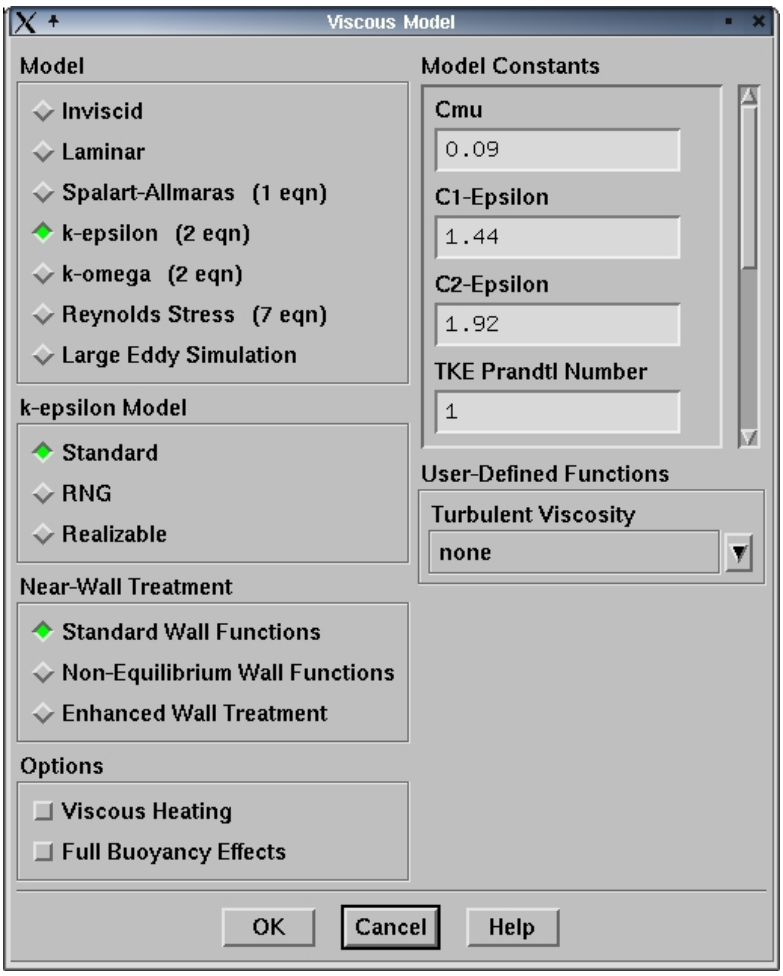

Enabling energy equation.

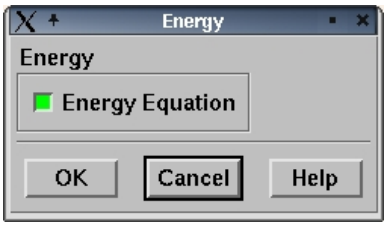

Select and turn on or off radiation model.

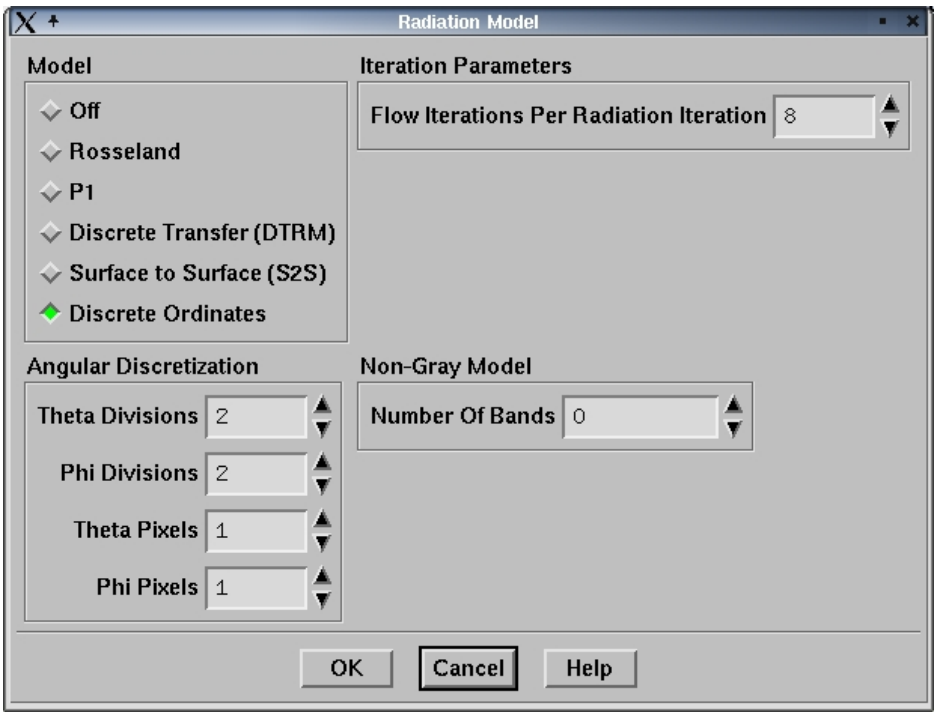

The window below defines chemistry model and turbulence-chemistry interaction model. If convergence difficulty is encountered, the option of “Diffusion Energy Source” could be disabled.

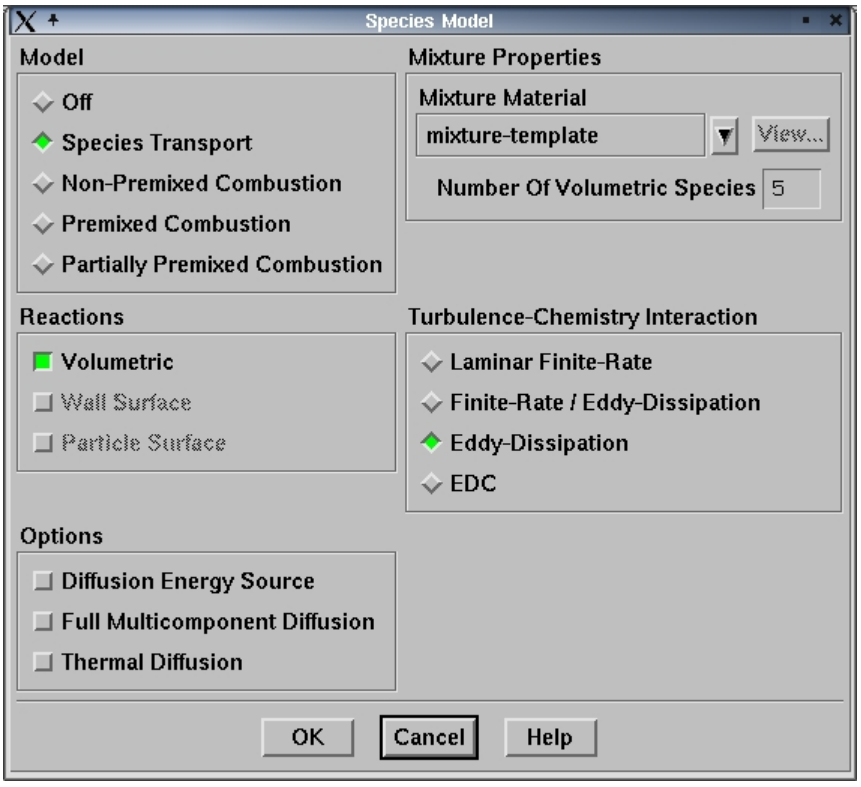

Step 3. Material definitions

The solids, fluids and mixture can be defined, respectively, by selecting in the drop-down list of “Material Type”.

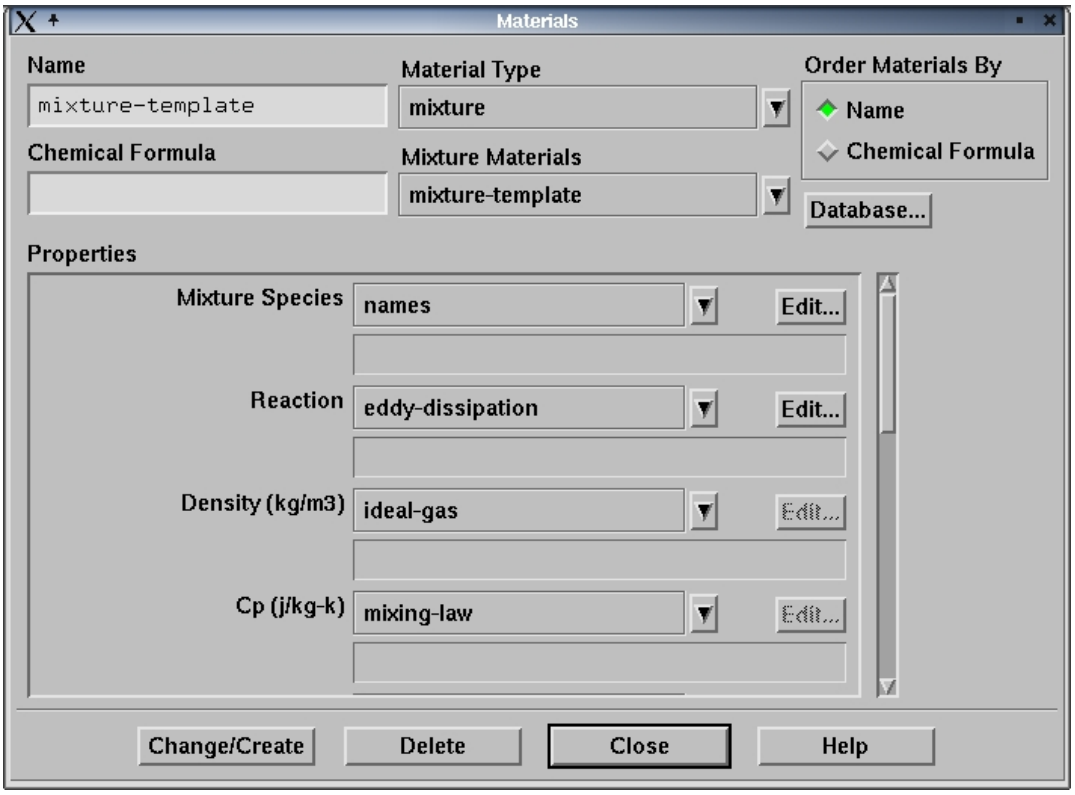

The under part of the “Properties” sub-window is shown below.

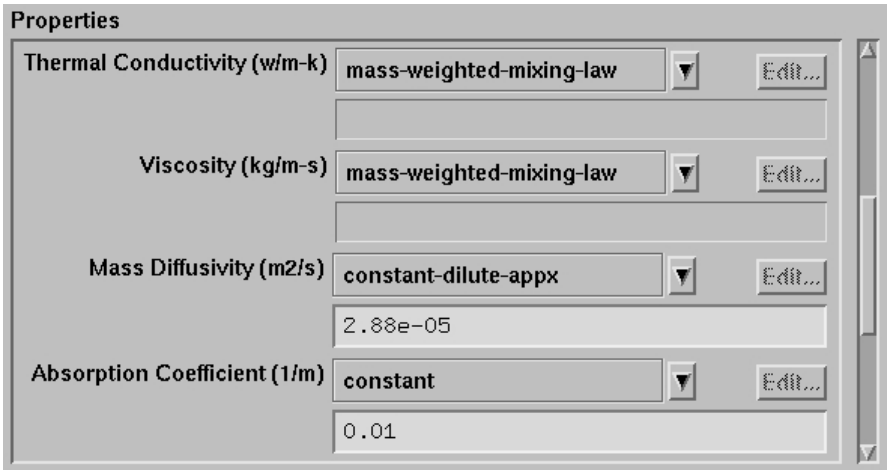

In the “Material” window, press “Edit” in the item of “Mixing Species” to select species. Normally nitrogen is put in the end for convenience.

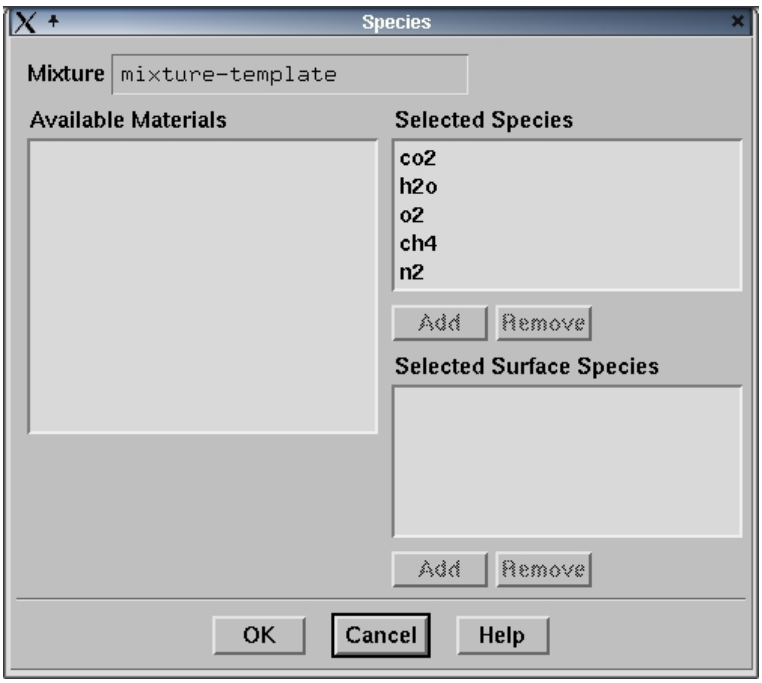

In the “Material” window, press “Edit” in the item of “Reaction” to define the eddy-dissipation model.

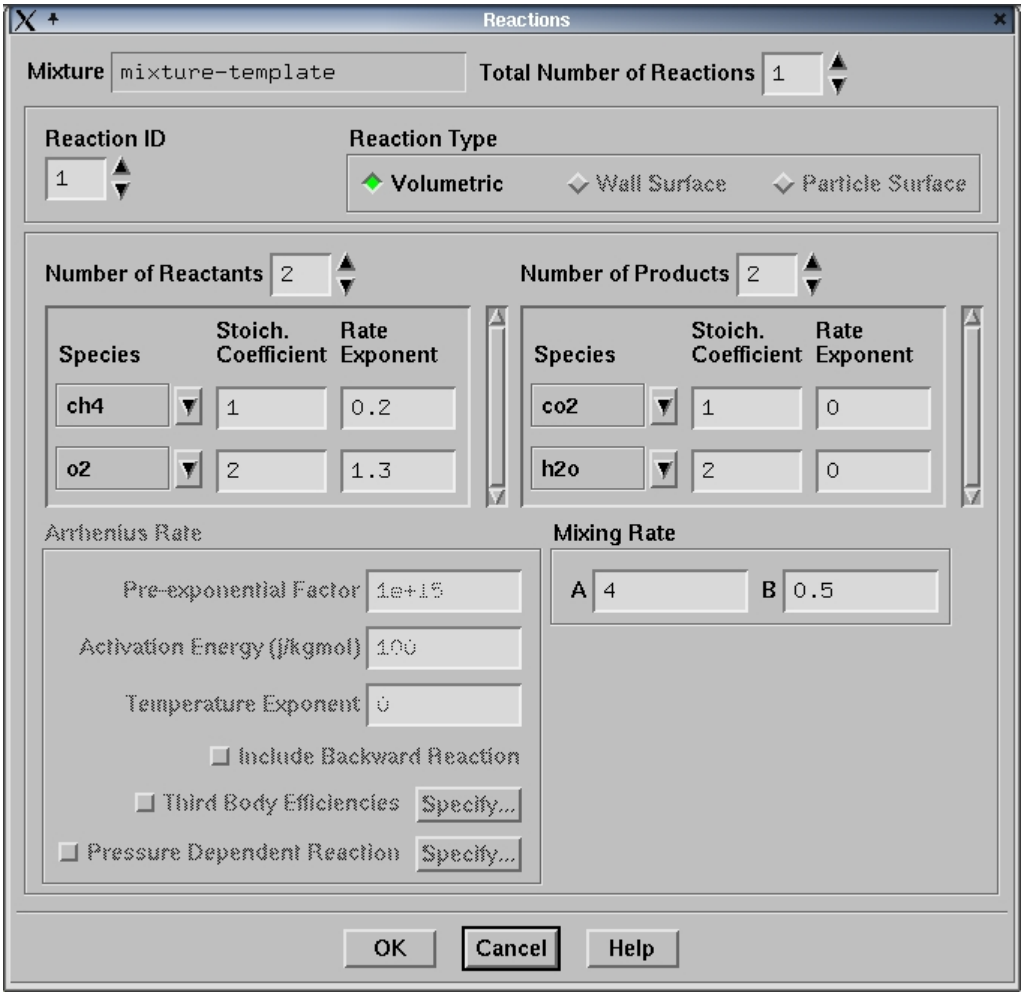

Step 4. Operating conditions

Operating pressure and temperature can be specified in this window. If the gravity is not very important in the problem, the option of “Gravity” can be disabled.

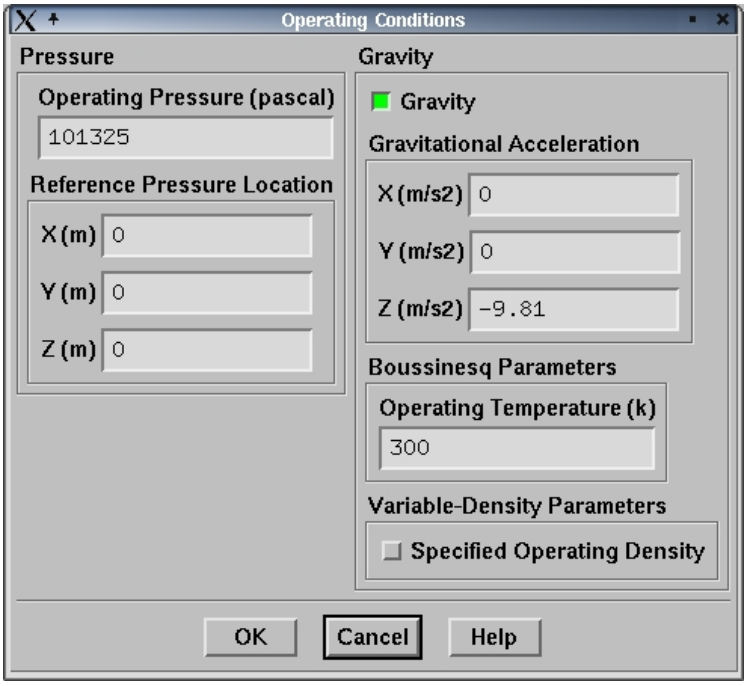

Step 5. Boundary conditions

In this window, the control volumes, walls, inlets, outlets, porous jumps and so on can be defined.

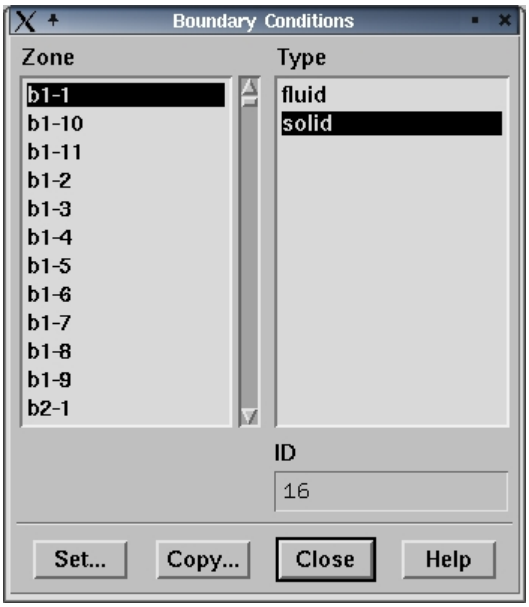

An example of the definition of a solid volume.

An example of the definition of a fluid volume.

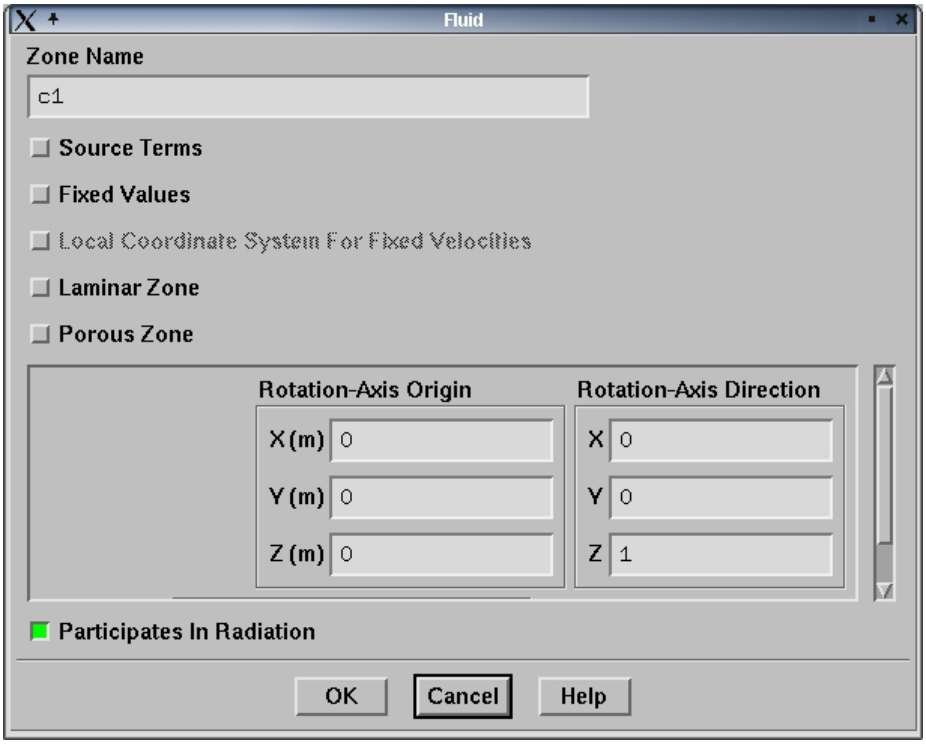

An example of the definition of an outside wall of the rotary kiln.

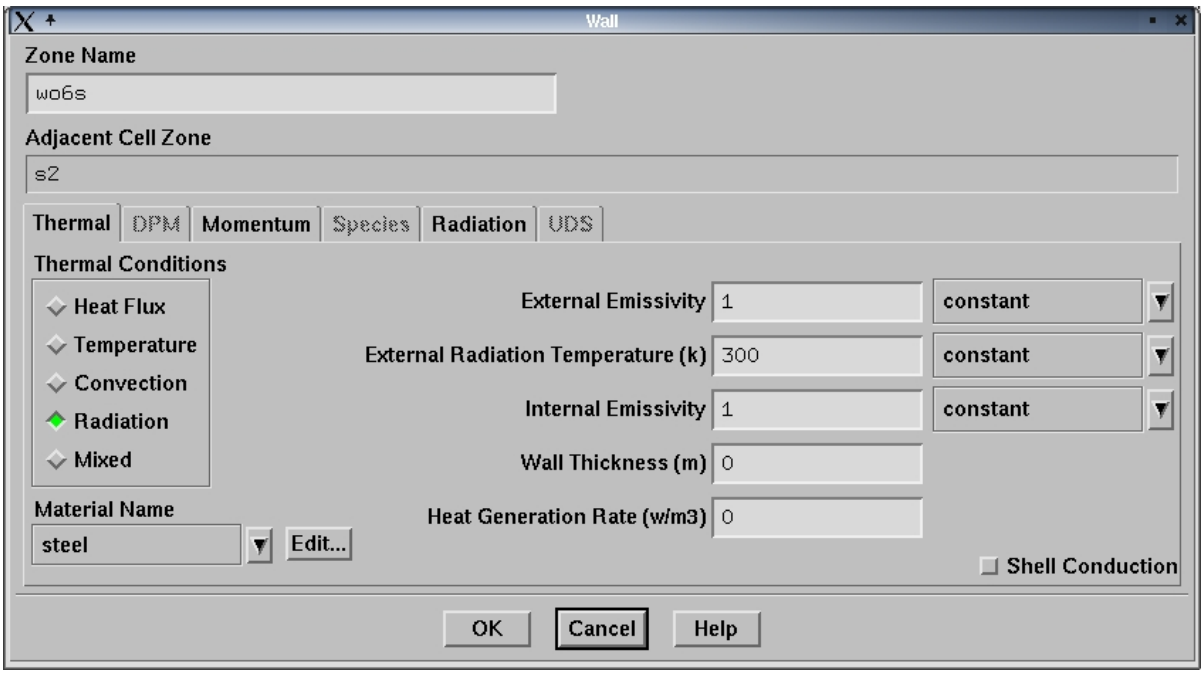

An example of the definition of a coupled wall in the rotary kiln. It is not necessary to define the other one being shadowed by this coupled wall.

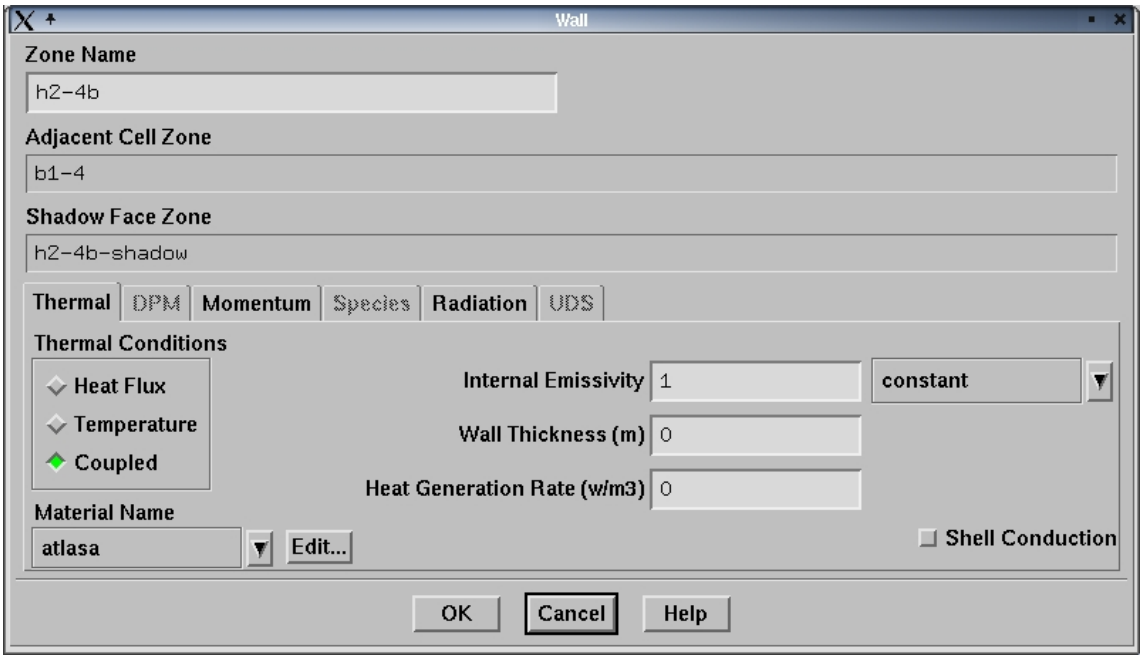

An example of the definition of a wall of the PCC.

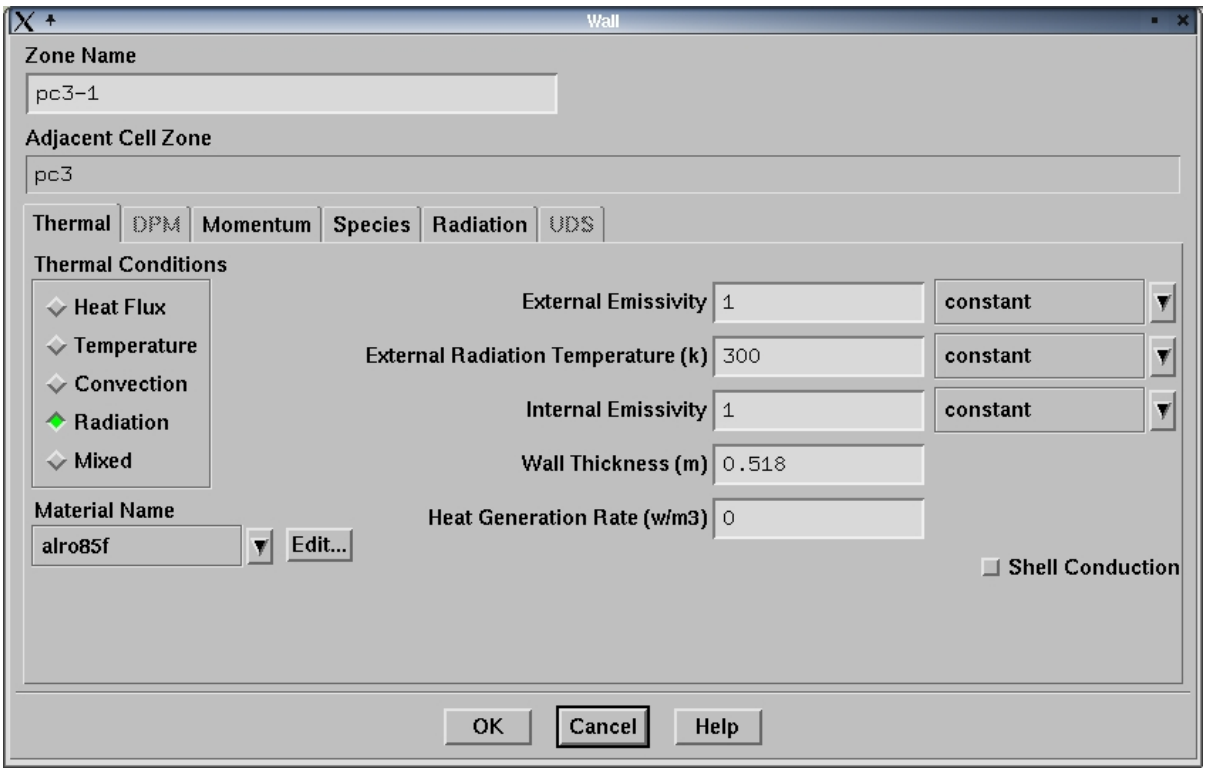

Methane injection boundary.

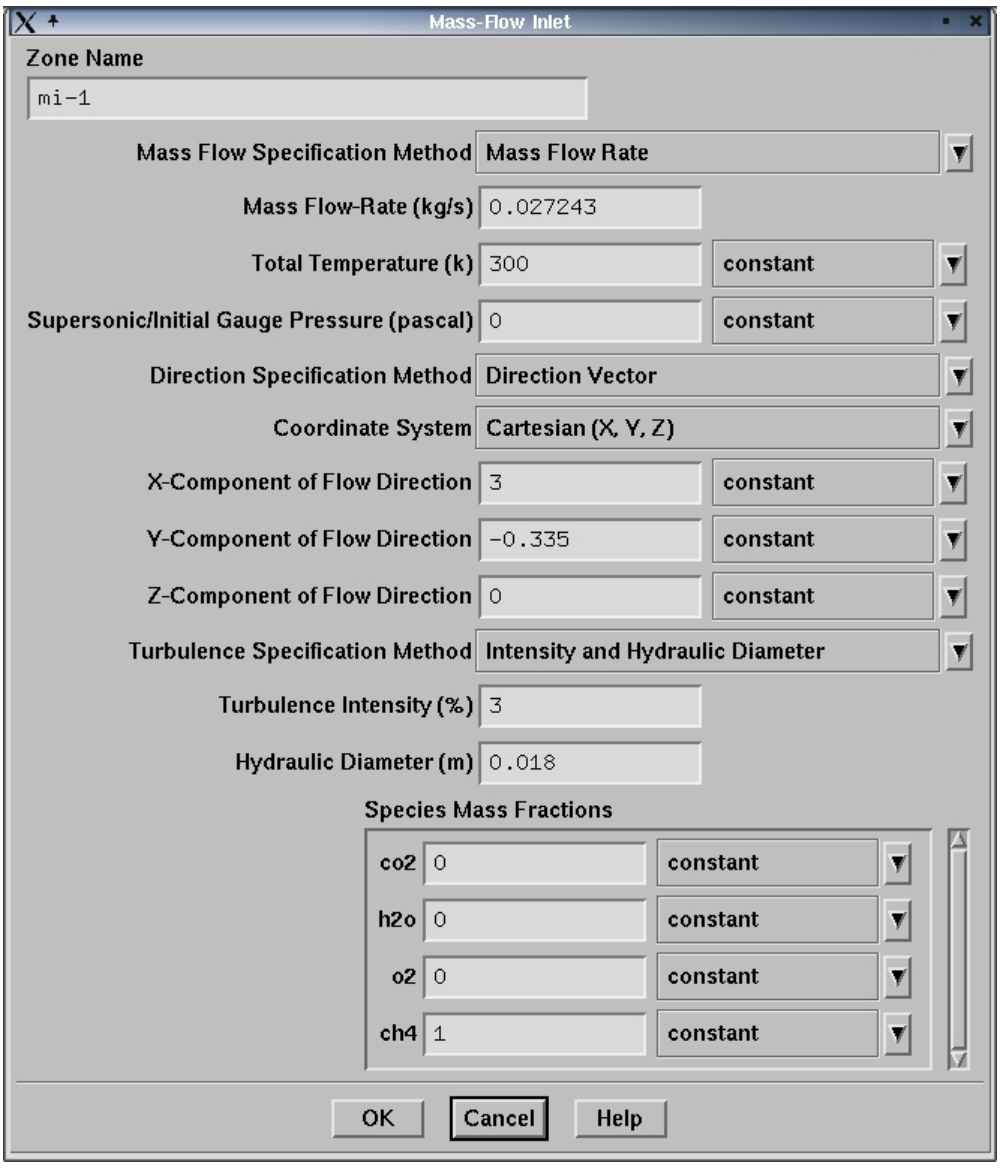

Air injection boundary.

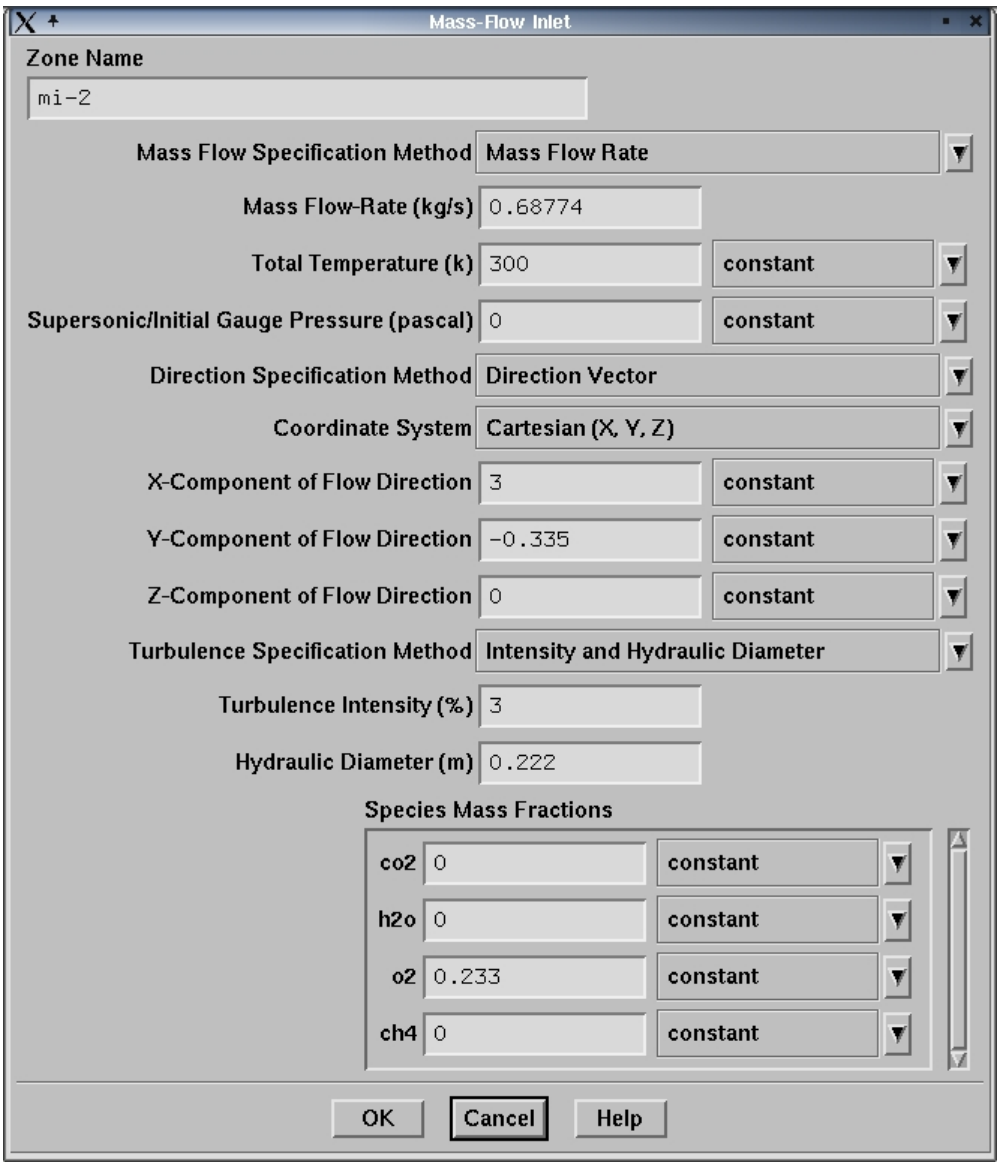

Water supply boundary.

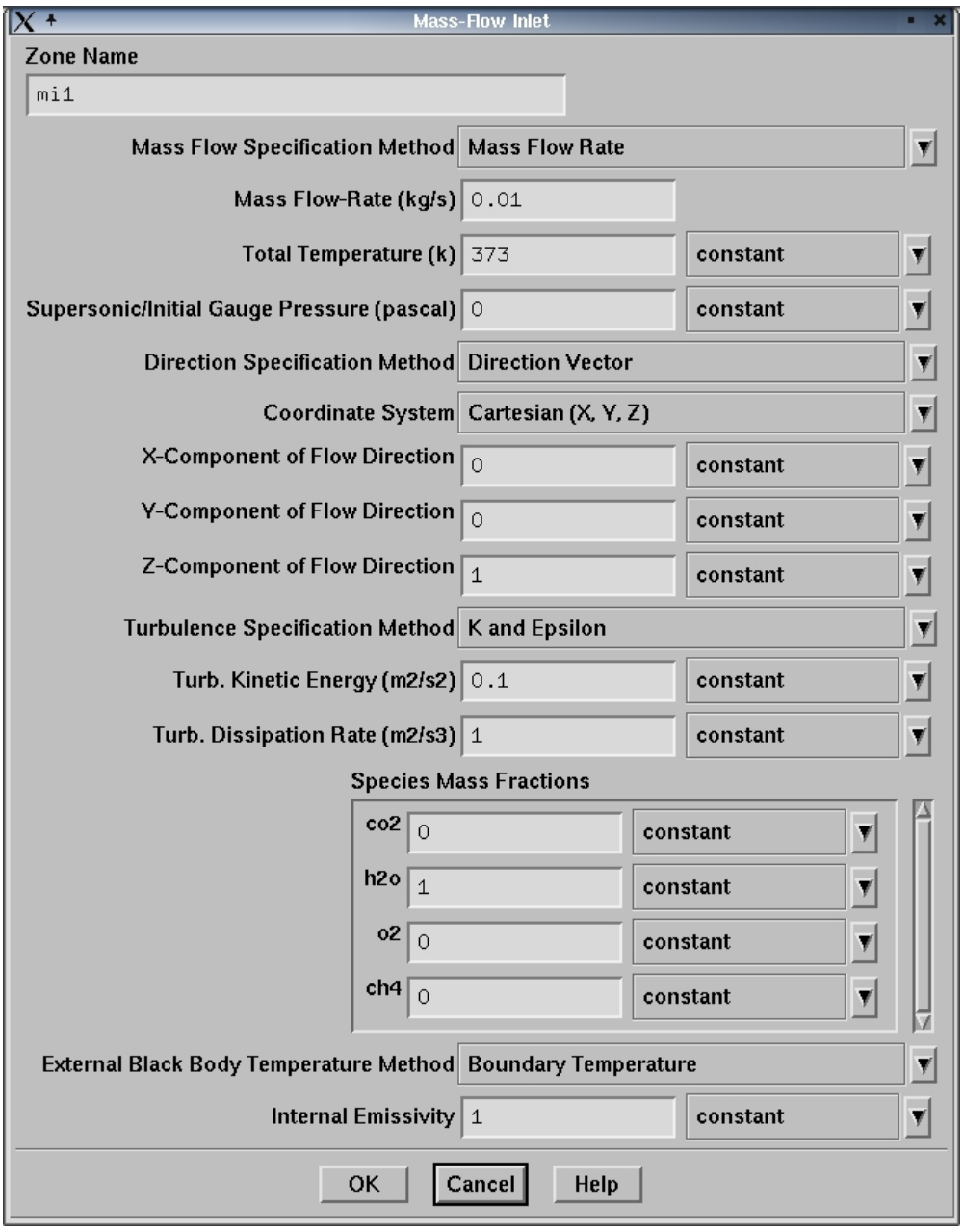

Pressure outlet boundary of the PCC.

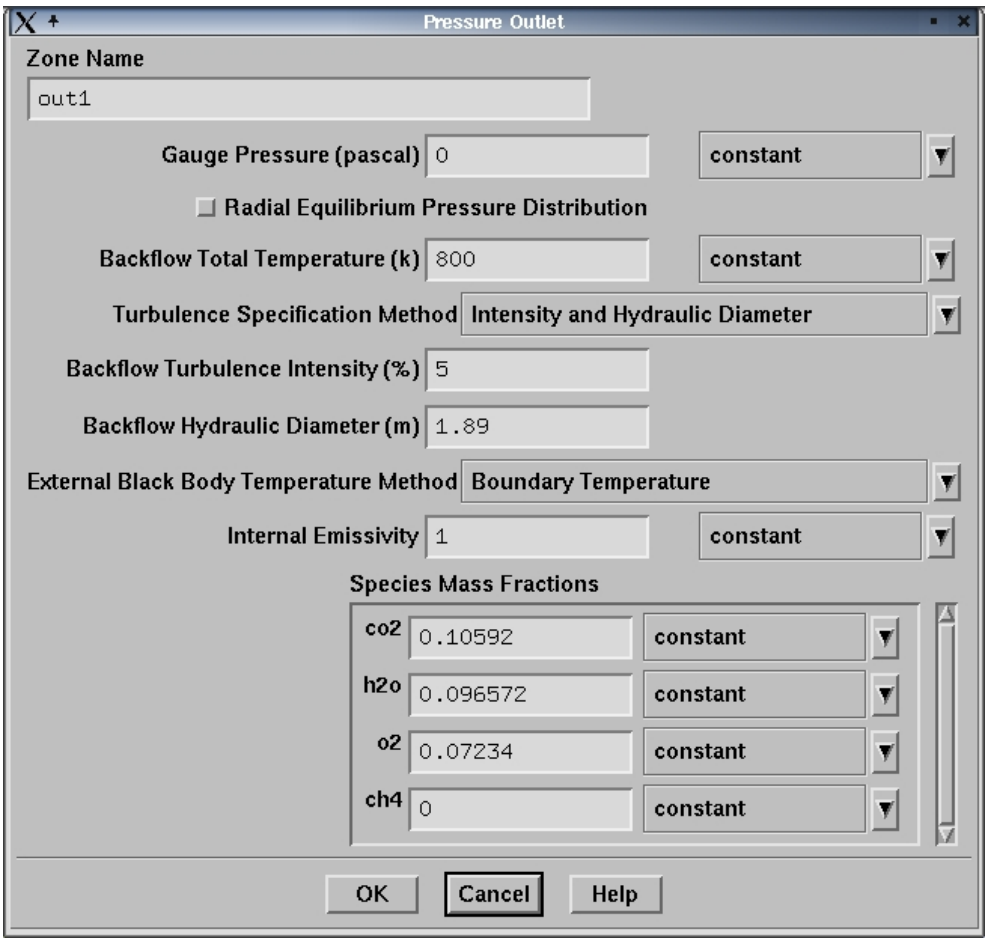

Inlet of the cooling system.

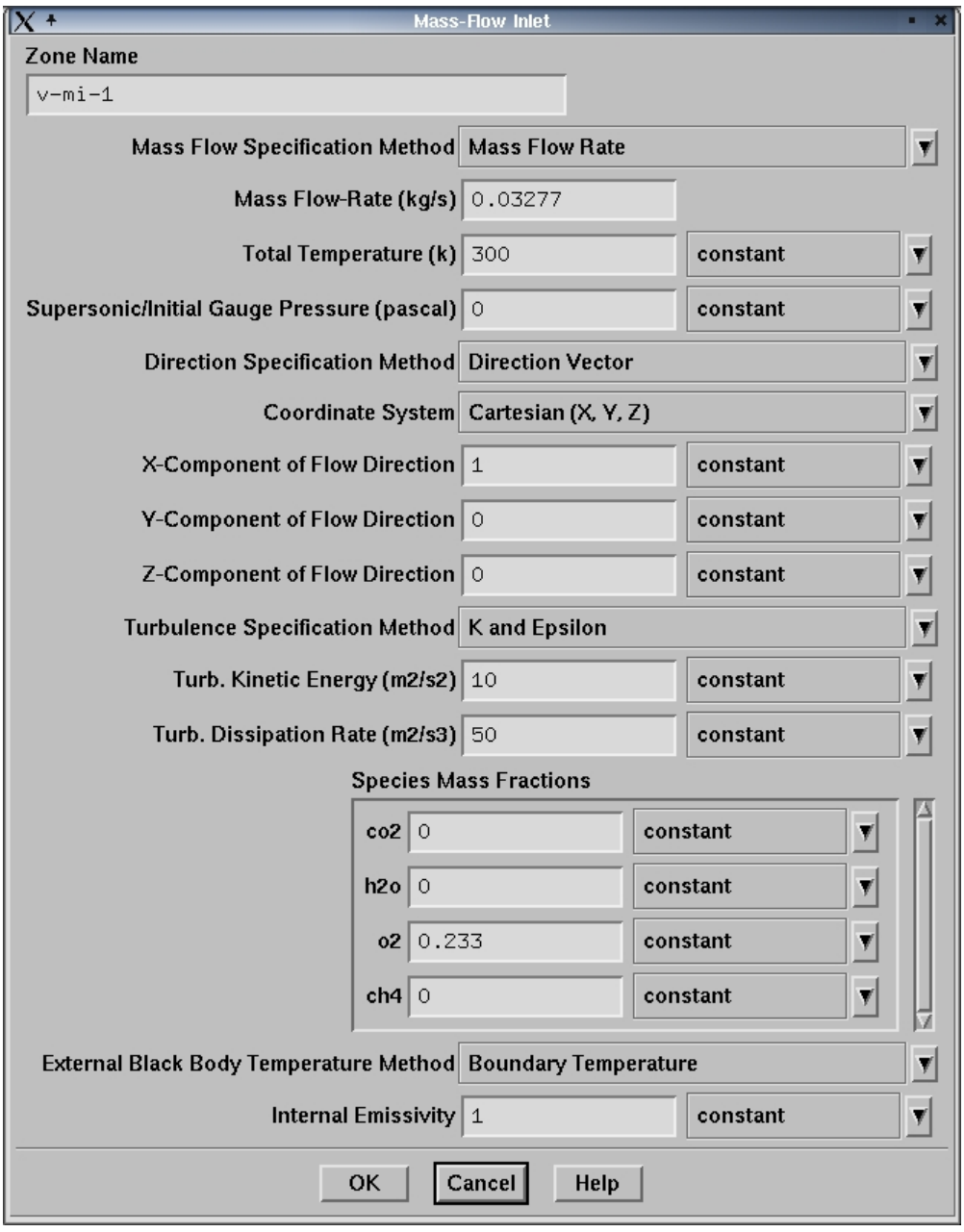

Outlet of the cooling system.

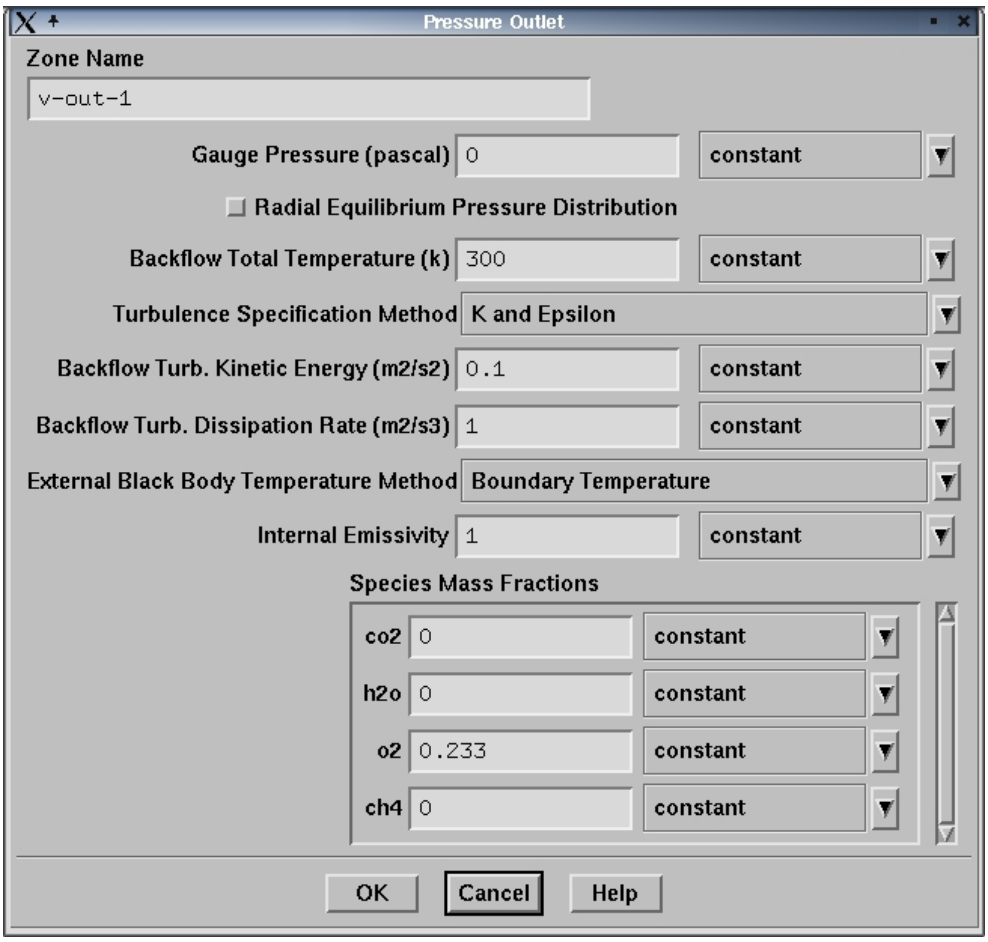

Settings of a porous jump.

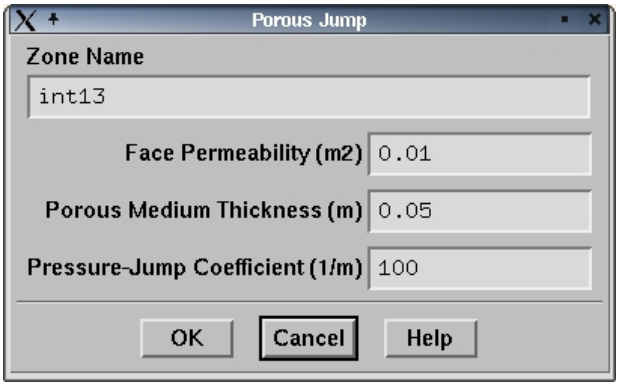

Step 6. Initialization

An initial guess of solution can be specified in this window, including initial velocities, turbulence parameters, mixture compositions, pressure and temperature.

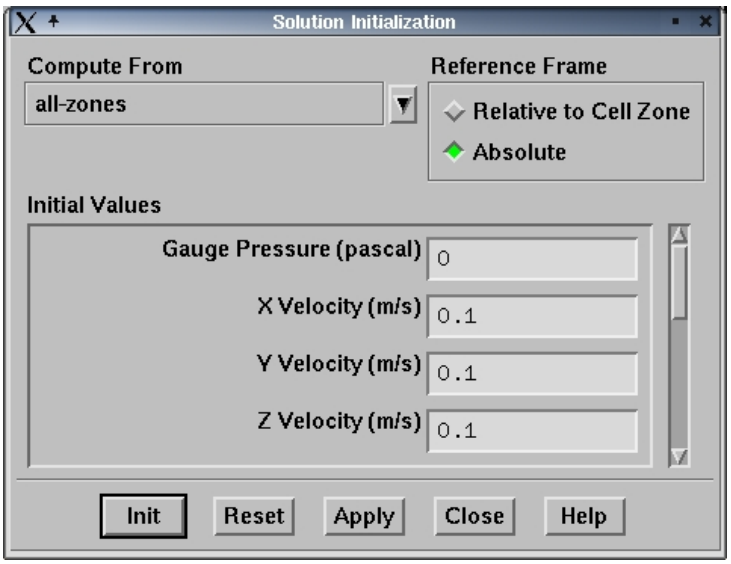

Step 7. Solution control

Equations can be turned on or off, under-relaxation factors and discretization schemes are specified here.

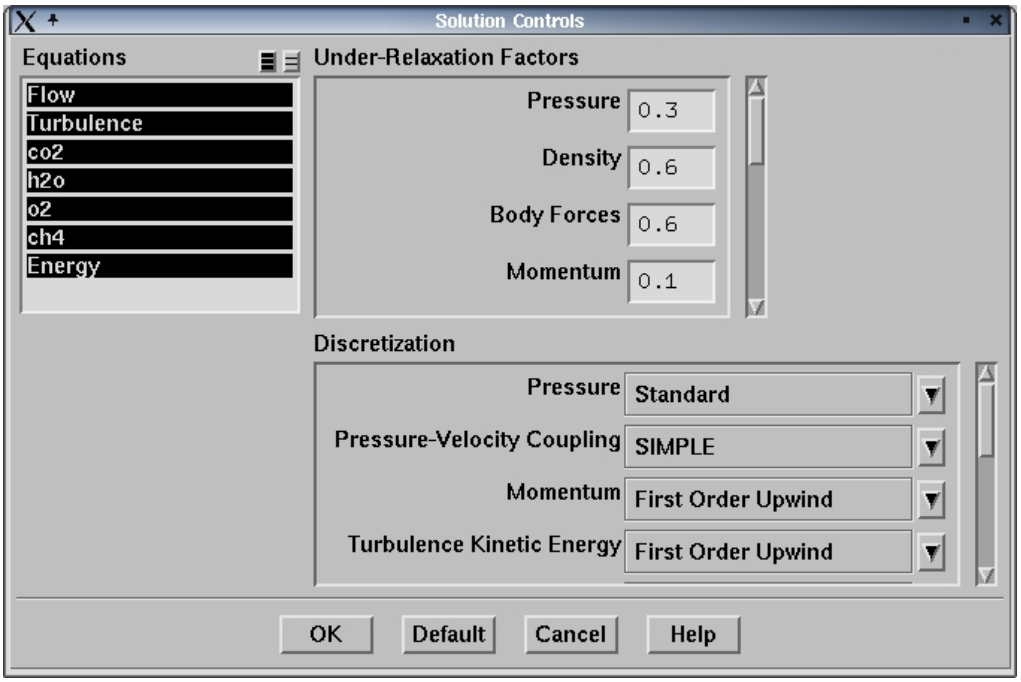

Step 8. Convergence-related monitors

First, turn on the residuals monitor.

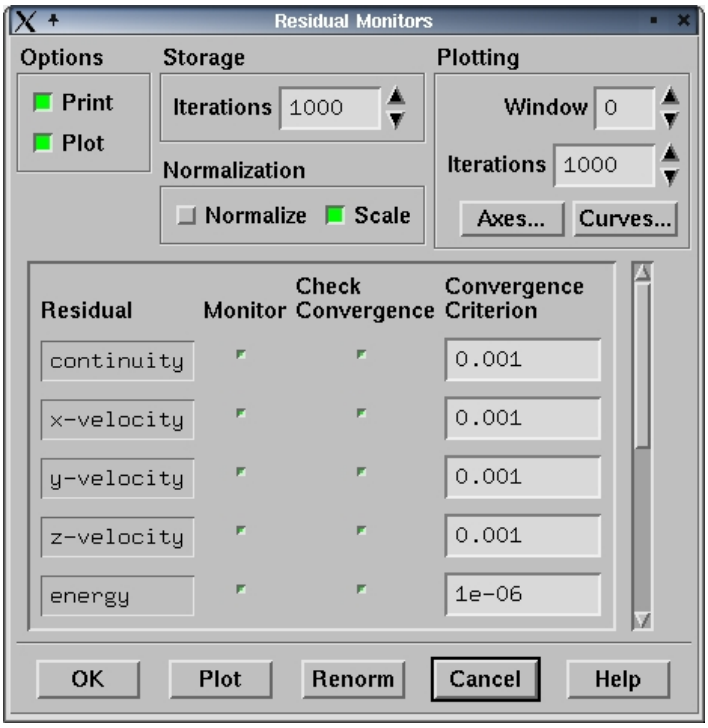

Second, monitor the coefficient of force, e.g., on the wall of pc31,

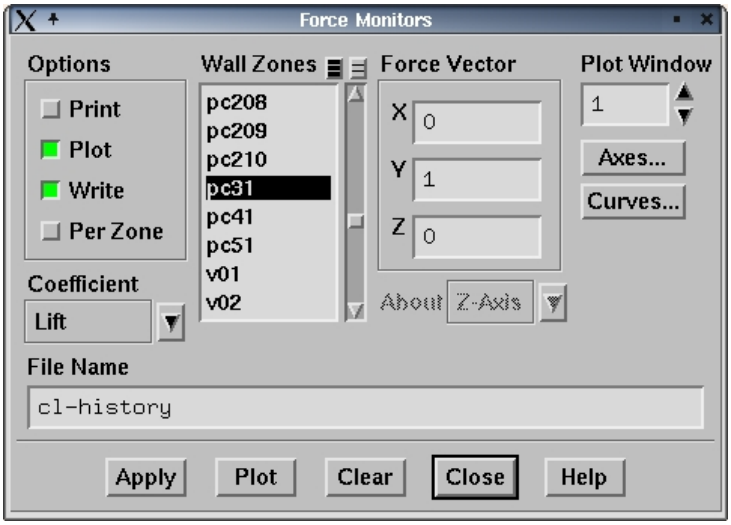

and/or, monitor some integrated quantities in some concerned volumes, e.g., density in volume of pc3.

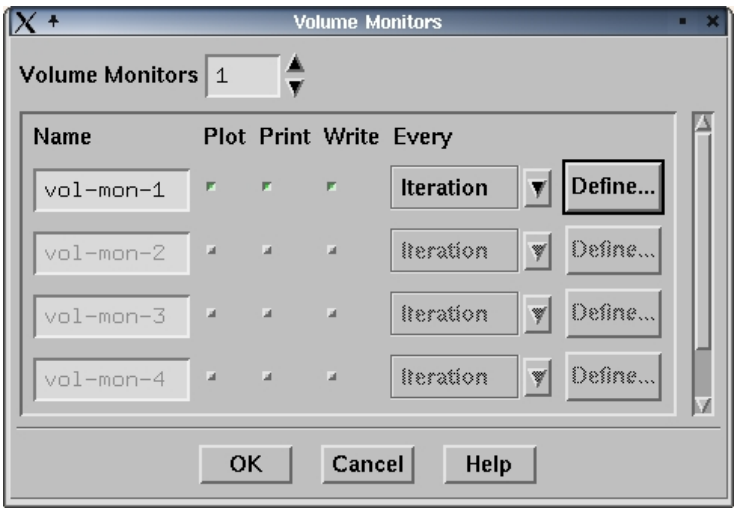

Press “Define” button in the window above, then define the concerned quantity in the concerned volumes in the window below.

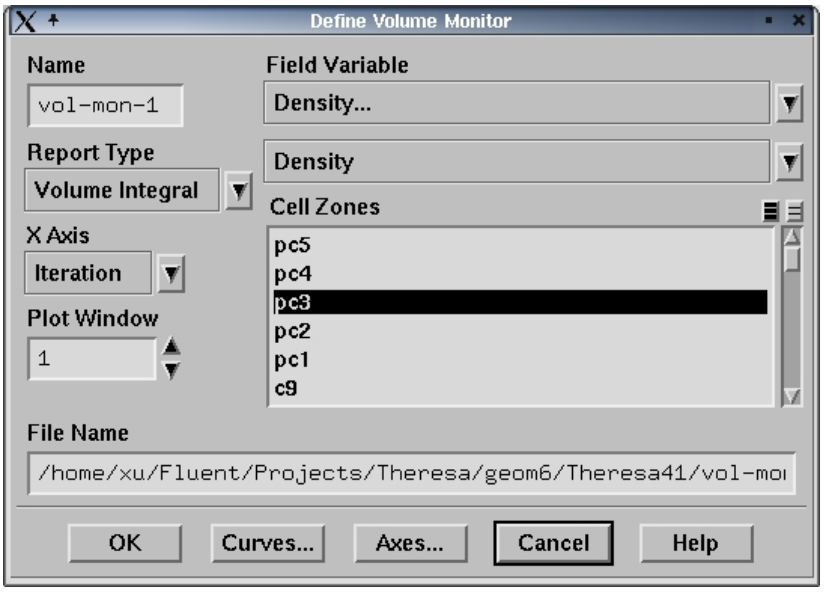

Step 9. Executes commands when calculating

For an instance, temperature distribution profiles and XY-plot are recorded in every five iterations for post-processing.

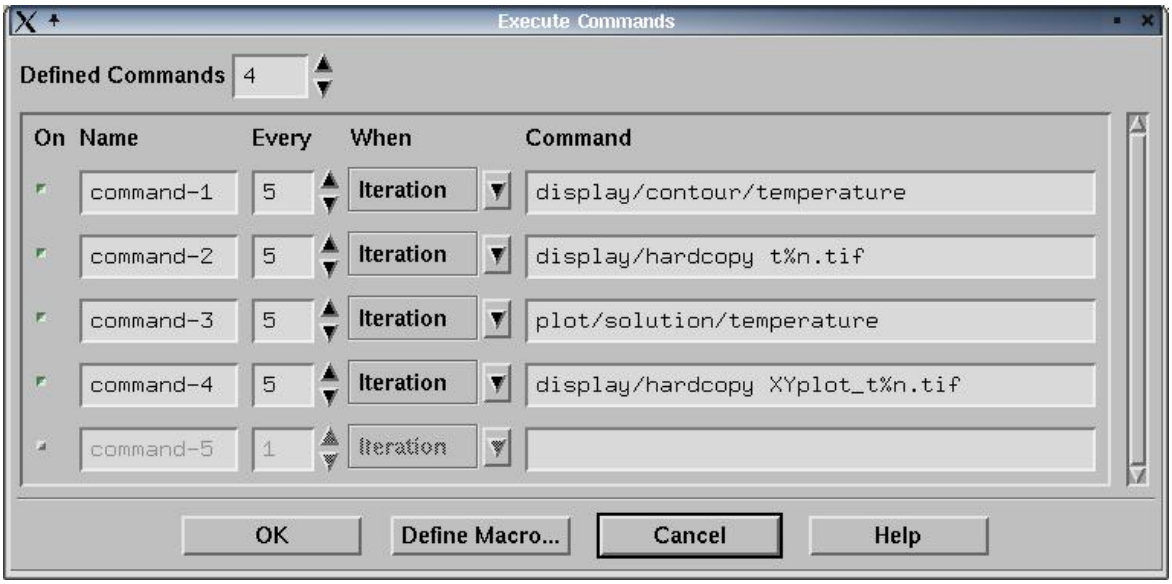

Step 10. Begin to iterate

Press “Iterate” to start the journey of searching the solution.